Syntheses and Characterization of Upper Rim 1,2- and 1,3-Diphosphinated Calix[4]arenes and Their Corresponding 1,5-Cyclooctadienylrhodium(I) Complexes: Comparison of the Catalytic Hydroformylation Properties of Terminal Alkenes

François Plourde, Karine Gilbert, Jonathan Gagnon,† and Pierre D. Harvey*

Département de Chimie, Université de Sherbrooke, Sherbrooke, P.Q., Canada, J1K 2R1

Received February 11, 2003

The 5,11- (1,2-isomer) and 5,17-bis(dialkylphosphino)-25,26,27,28-tetra-*n*-propoxycalix[4]-arene (1,3-isomer) ligands (alkyl = Me, *i*-Pr) have been prepared and coordinated to Rh-$(COD)^+$ fragments (COD = 1,5-cyclooctadiene). The ligands 5,17-bis(diphenylphosphino)-11,23-dibromo-25,26,27,28-tetra-*n*-propoxycalix[4]arene and 5,11-bis(diphenylphosphino)-25,26,27,28-tetra-*n*-propoxycalix[4]arene have been coordinated to $M(COD)^+$ (M = Rh, Ir) and RhCl(CO) fragments, as well. On the basis of mass spectrometry and ^{31}P NMR spin−lattice relaxation time measurements (T_1), all of the complexes are found to be dimers. Molecular modeling provides evidence that ring stress favors the dimer over the monomer, and the modeled structures for both 1,2- and 1,3-isomers have been corroborated by the comparison of the photophysics of the $Ir(COD)^+$ species at 77 K. The decrease in emission lifetimes of the $P_2Ir(C{=}C)_2^+$ lumophore in the presence of 1-hexene is more pronounced for the 1,3-isomer, indicating reduced steric hindrance about the metallic center. The catalytic hydroformylation of five terminal alkenes using all six $Rh(COD)^+$ catalyst precursors has been investigated under various conditions in order to extract the turnover frequencies (tof as defined as the number of moles of products divided by the total number of moles of rhodium used per hour) and the ratios of the product distribution (*n*/*i*, normal vs internal). The comparison of the data suggests that the basicity and the cone angle of the phosphines influence the *n*/*i* ratios. The tof's are generally larger for the 1,2-series for 1-hexene, but depend on the nature of the phosphine for styrene, vinyl acetate, vinyl benzoate, and vinyl *p*-*tert*-butylbenzoate. All in all, these complexes are good catalysts with respect to literature data, notably those containing the $(i\text{-}Pr_2P)-$ groups. During the course of this study, one hydride carbonyl complex has been synthesized and characterized from ^1H and ^{31}P NMR, IR, and T_1 measurements.

Introduction

The syntheses and investigations of calixarenes and related derivatives continue to be a very active field.[1] Although applications of such molecules for cation extractions, biomimetics, luminescence probes, sensors, and nuclear waste treatment are well known,[1b] their uses in homogeneous catalysis are more limited, concentrating mainly on lower rim functionalized calix[4]-arenes.[1a,2] Recently, numerous works in the area of rhodium-catalyzed hydroformylation reactions[3] have focused on parameters influencing the mechanism and the product distribution (*n*/*i* ratio) such as the phosphine cone angle and bulkiness,[4] the diphosphine natural bite angle,[5] the chirality,[6] and the diphosphine electronic effects.[7] With respect to diphosphine bite angle, angles approaching 90° and 120° favor coordination at the

* To whom correspondence should be addressed. Fax: (819) 821-8017. Tel: (819) 821-7092 or (819) 821-8000, ext. 2005. E-mail: pharvey@USherbrooke.ca.

† Current address: Département de Chimie, Université du Québec à Rimouski.

(1) (a) Asfari, Z.; Börner, V.; Harrowfield, J.; Vicens, J. *Calixarenes 2001*; Kluwer Academic Publishers: Dordrecht, 2001. (b) Gutsche, C. D. *Calixarene Revisited*; Royal Society of Chemistry: Cambridge, U.K., 1998.

(2) See for examples: (a) Kunze, C.; Selent, D.; Neda, I.; Schmutzler, R.; Spannenberg, A.; Börner, A. *Heteroat. Chem.* **2001**, *12*, 577. (b) Parlevliet, F. J.; Kiener, C.; Fraanje, J.; Goubitz, K.; Lutz, M.; Spek, A. L.; Kamer, P. C. J.; van Leeuwen, P. W. N. M. *J. Chem. Soc., Dalton Trans.* **2000**, 1113. (c) Cobley, C. J.; Ellis, D. D.; Orpen, A. G.; Pringle, P. G. *J. Chem. Soc., Dalton Trans.* **2000**, 1109. (d) Dieleman, C.; Steyer, S.; Jeunesse, C.; Matt, D. *J. Chem. Soc., Dalton Trans.* **2001**, 2508. (e) Steyer, S.; Jeunesse, C.; Matt, D.; Welter, R.; Wesolek, M. *J. Chem. Soc., Dalton Trans.* **2002**, 4264.

(3) (a) van Leeuwen, P. W. N. M.; Claver, C. *Rhodium Catalysed Hydroformylation*; Kluwer Academic Publishers: Dordrecht, 2000. (b) Ungvàry, F. *Coord. Chem. Rev.* **1999**, *188***,** 263. (c) Ungvàry, F. *Coord. Chem. Rev.* **1998**, *170*, 245. (d) Ungvàry, F. *Coord. Chem. Rev.* **1997**, *167*, 233. (e) Beller, M.; Cornils, B.; Frohning, C. D.; Kohlpaintner, C. W. *J. Mol. Catal. A* **1995**, *104*, 17.

(4) See for instance: (a) Trzeciak, A. M.; Glowiak, T.; Grzybek, R.; Ziolkowski, J. J. *J. Chem. Soc., Dalton Trans.* **1997**, 1831. (b) van Rooy, A.; Kamer, P. C. J.; van Leeuwen, P. W. N. M.; Goubitz, K.; Fraanje, J.; Veldman, N.; Spek, A. L. *Organometallics* **1996**, *15*, 835. (c) Agbossou, F.; Carpentier, J. F.; Mortreux, A. *Chem. Rev.* **1995**, *95*, 2485.

10.1021/om030095o CCC: $25.00
Publication on Web 06/10/2003

apical-equatorial (ea) and diequatorial positions (ee), respectively, of the triangular bipyramidal intermediates.

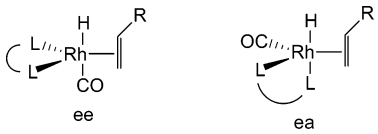

By examining the structural features of square-planar and octahedral transition metals complexed onto the upper rim of the 1,3-bis(diphenylphosphino)calix[4]-arene reported by Matt and co-workers (**1** and **2**),[8] a rhodium intermediate exhibiting a diapical coordination appears highly plausible. However steric hindrance may slow the rates of reactions. To our knowledge, the diapical case has not been reported and certainly deserves exploration.

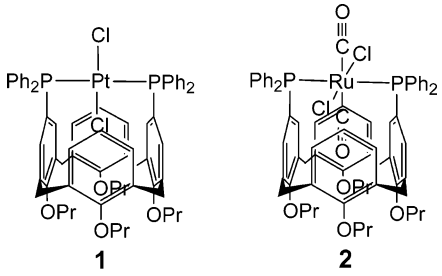

We now wish to report the syntheses of four new diphosphinated calix[4]arene ligands, 1,3- and 1,2-bis-(diisopropylphosphino)calix[4]arene, and -bis(dimethylphosphino)calix[4]arene, and their corresponding Rh(COD)$^+$ catalytic precursors (COD = 1,5-cyclooctadiene) as well as their 1,3- and 1,2-bis(diphenylphosphino)-calix[4]arene analogues, which exist as dimers. Molecular modeling suggests that the diapical coordination is strongly favored. A comparative study of hydroformylation reactions of five terminal alkenes indicates differences between the two types of isomers.

Experimental Section

Materials. The following products have been purchased: acetone (ACP), argon (Praxair), *n*-butyllithium (Aldrich), *tert*-butyllithium (Aldrich), chlorodiisopropylphosphine (Aldrich), chlorodimethylphosphine (Aldrich), chloroform (Anachemia), carbon monoxide (Praxair), COD (Aldrich), dichloromethane (ACP), ethanol (Les alcools de commerce inc.), ethyl acetate (ACP), hexanes (ACP), 1-hexene (Aldrich), hydrogen (Praxair), hydrogen peroxide (Fisher), methylcyclohexane (BDH), dinitrogen (Praxair), phenylsilane (Aldrich), silver(I) hexafluorophosphate (Aldrich), styrene (Aldrich), thallium hexafluorophosphate (Aldrich), tetrahydrofuran (Anachemia), toluene (Anachemia), trichloroiridium(III) hydrate (Pressure Chem. Co.), trichlororhodium(III) hydrate (Pressure Chem. Co.), vinyl acetate (Aldrich), vinyl benzoate (Aldrich), and vinyl *tert*-butylbenzoate (Aldrich). 5,17-Dibromo-25,26,27,28-tetra-*n*-propoxycalix[4]arene (**3**),[9] 5,17-dibromo-11,23-diphenylphosphino-25,26,27,28-tetra-*n*-propoxycalix[4]arene (**5c**),[9a] 5,11-dibromo-25,26,27,28-tetra-*n*-propoxycalix[4]arene[9a] (**7**), 5,11-bis(diphenylphosphino)-25,26,27,28-tetra-*n*-propoxy-calix-[4]arene[9a] (**9c**), and bis[chloro(1,5-cyclooctadienyl)rhodium-(I)][10] were synthesized according to literature procedures. All solvents were freshly distilled before use. All air- or moisture-sensitive materials were handled using standard Schlenk techniques, high-vacuum manifolds, and inert atmosphere in a glovebox. Column chromatography was performed on 230−400 mesh silica gel (60 Å).

Apparatus. All NMR spectra were acquired with a Bruker AC-300 spectrometer (^{1}H 300.15 MHz, ^{13}C 75.48 MHz, ^{31}P 121.50 MHz) using the solvent as chemical shift standard, except in ^{31}P NMR, where the chemical shifts are relative to D_3PO_4 85% in D_2O. All chemical shifts (δ) and coupling constants (J) are given in ppm and hertz, respectively. The IR spectra were acquired on a Perkin-Elmer FT-IR 1600 series spectrometer. The UV−vis spectra were acquired on a Hewlett-Packard diode array spectrophotometer 8452A model. The emission and excitation spectra were obtained using a PTI LS100 spectrometer. The emission lifetimes were measured with a nanosecond N_2 laser system from PTI model GL-3300 pumping a dye laser model GL-302. The excitation wavelength was 500 nm using the PLD500 C-500 dye. Electronic ionization mass spectra were obtained on a VG Instruments ZAB-IF spectrometer at a potential of 70 eV. Fast atom bombardment mass spectra were acquired at the Université de Montréal. MALDI-TOF mass spectra were acquired from a Bruker Proflex III linear mode spectrometer with a nitrogen laser (337 nm) from the Université de Bourgogne in Dijon (France) with a dithranol matrix. Analytical gas chromatography was performed on a Hewlett-Packard 5890 series II spectrometer coupled with a HP 5971 series selective mass detector. Elementary analyses were performed at the Université de Montréal.

5,17-Bis(dimethylphosphinoyl)-25,26,27,28-tetra-*n*-propoxycalix[4]arene (4a) (Cone). A solution of 100 mg (0.13 mmol) of **3** in 5 mL of dry THF at −78 °C was treated with a solution of 0.18 mL (0.30 mmol) of *n*-BuLi 1.6 M in hexane. The solution was stirred for 1 h at −78 °C as 0.1 mL (0.65 mmol) of Me_2PCl was added. The solution was stirred for an additional 20 h and was allowed to reach room temperature. A 0.1 mL (0.88 mmol) portion of hydrogen peroxide (30% in water) was then added, and the mixture stirred for 1 h. The solvent was evaporated and the yellow residue was purified using column chromatography under inert atmosphere using a 10:90 ethanol/$CHCl_3$ mixture (R_f = 0.25). A white solid was obtained. Yield: 20% (21 mg); T_m = 280 °C; IR (neat solid) ν(P=O) = 1206 cm^{-1}; ^{1}H NMR ($CDCl_3$) 7.42 (d, 4H, J = 11.60, Ph), 6.23 (t, 2H, J = 7.54, Ph), 6.07 (d, 4H, J = 7.55, Ph), 4.45 (d, 4H, J = 13.42, ArCH_2), 4.05 (t, 4H, J = 6.60, OCH_2), 3.68 (t, 4H, J = 6.81, OCH_2), 3.20 (d, 4H, J = 13.53, ArCH_2), 1.90 (m, 8H, CH_2CH_3), 1.76 (d, 12H, J = 12.88, $P(CH_3)_2$), 1.08 (t, 6H, J = 7.40, CH_2CH_3), 0.89 (t, 6H, J = 7.43, CH_2CH_3); ^{13}C {^{1}H} NMR ($CDCl_3$) 160.92, 155.29, 137.20 (d, J_{C-P} = 13.9, C_{Ar}−P), 132.78, 130.12, 129.99, 127.77, 122.48, 76.99, 76.81, 30.93, 23.20 (d, J_{C-P} = 21.1, CH_3−P), 18.38, 17.42, 10.67, 9.85; ^{31}P{^{1}H} NMR ($CDCl_3$) 38.37 (s); MS (FAB): 745

(5) (a) Casey, C. P.; Whiteker, G. T.; Melville, M. G.; Petrovich, L. M.; Gavney, J. A.; Powell, D. R. *J. Am. Chem. Soc.* **1992**, *114*, 5535. (b) Casey, C. P.; Petrovich, L. M. *J. Am. Chem. Soc.* **1995**, *117*, 6007. (c) Kranenbrug, M.; van der Burgt, Y. E. M.; Kamer, P. C. J.; van Leeuwen, P. W. N. M.; Goubitz, K.; Fraanje, J. *Organometallics* **1995**, *14*, 3081.

(6) See for instance: Horiuchi, T.; Shirakawa, E.; Nozaki, K.; Takaya, H. *Organometallics* **1997**, *16*, 2981.

(7) (a) Casey, C. P.; Paulsen, E. L.; Beuttenmueller, E. W.; Proft, B. R.; Petrovich, L. M.; Matter, B. A.; Powell, D. R. *J. Am. Chem. Soc.* **1997**, *119*, 11817. (b) Casey, C. P.; Paulsen, E. L.; Beuttenmueller, E. W.; Proft, B. R.; Matter, B. A.; Powell, D. R. *J. Am. Chem. Soc.* **1999**, *121*, 63.

(8) (a) Wieser-Jeunesse, C.; Matt, D.; DeCian, A. *Angew. Chem., Int. Ed.* **1998**, 2861. (b) Lejeune, M.; Jeunesse, C.; Matt, D.; Kyritsakas, N.; Wleter, R.; Kintzinger, J.-P. *J. Chem. Soc., Dalton Trans.* **2002**, 1642.

(9) (a) Gagnon, J.; Vézina, M.; Harvey, P. D. *Can. J. Chem.* **2001**, *79*, 1439. (b) Larsen, M.; Jorgensen, M. *J. Org. Chem.* **1996**, *61*, 6651.

(10) Giordano, G.; Crabtree, R. H. *Inorg. Synth.* **1989**, *28*, 88.

(M^+). Anal. Calcd for $C_{44}H_{58}O_6P_2$: C, 70.95; H, 7.79. Found: C, 69.84; H, 8.09.

5,17-Bis(diisopropylphosphinoyl)-25,26,27,28-tetra-*n*-propoxycalix[4]arene (4b) (Cone). This compound was prepared according to the same procedure described for **4a** using *i*-Pr_2PCl as phosphinating agent. A white solid was obtained. Yield: 55%; T_m = 222−225 °C; IR (neat solid): ν(P=O) = 1206 cm^{-1}; ^1H NMR (CD_2Cl_2) 7.66 (d, 4H, J = 12.00, Ph), 6.20 (t, 2H, J = 7.62, Ph), 5.96 (d, 4H, J = 7.64, Ph), 4.49 (d, 4H, J = 13.60, ArCH_2), 4.18 (t, 4H, J = 8.10, OCH_2), 3.65 (t, 4H, J = 6.72, OCH_2), 3.31 (d, 4H, 13.69, ArCH_2), 3.05 (m, 4H, P$CH(CH_3)_2$), 1.90 (m, 8H, CH_2CH_3), 1.53 (d, 6H, J = 7.00, PCH(CH_3)$_2$), 1.47 (d, 6H, J = 7.03, PCH(CH_3)$_2$), 1.40 (d, 6H, J = 7.12, PCH(CH_3)$_2$), 1.34 (d, 6H, J = 7.12, PCH(CH_3)$_2$), 1.08 (t, 6H, J = 7.20, CH_2CH_3), 0.89 (t, 6H, J = 7.40, CH_2CH_3); $^{13}C\{^1H\}$ NMR ($CDCl_3$) 163.94, 155.08, 139.45 (d, J_{C-P} = 12.5, C_{Ar}−P), 134.81, 134.70, 131.77, 127.35, 122.46, 77.28, 77.00, 30.67, 23.29 (d, J_{C-P} = 16.1, $(CH_3)_2CH$−P), 20.97, 20.39, 17.32, 16.44, 10.75, 9.64; $^{31}P\{^1H\}$ NMR (CD_2Cl_2) 29.57 (s); MS (FAB) 857 (M^+). Anal. Calcd for $C_{52}H_{74}O_6P_2$: C, 72.88; H, 8.64. Found: C, 72.74; H, 8.73.

5,17-Bis(dimethylphosphino)-25,26,27,28-tetra-*n*-propoxycalix[4]arene (5a) (Cone). A 40 mg (0.056 mmol) sample of **4a** was dissolved in 5 mL of toluene under an inert atmosphere. The solution was refluxed, and 0.2 mL (1.62 mmol) of phenylsilane was added. The solution was stirred and refluxed for 12 h. The solvent was then evaporated, and the crude product was purified using column chromatography under inert atmosphere using a 5:95 ethyl acetate/hexane mixture (R_f = 0.38). A white solid was obtained (41 mg). Yield: 105%; T_m = 204−206 °C; ^1H NMR (CD_2Cl_2) 7.06 (d, 4H, J = 7.35, Ph), 6.26 (m, 6H, Ph), 4.43 (d, 4H, J = 13.21, ArCH_2), 3.97 (t, 4H, J = 8.03, OCH_2), 3.71 (t, 4H, J = 7.02, OCH_2), 3.15 (d, 4H, J = 13.28, ArCH_2), 1.93 (t of q (∼sext), 4H, J = 7.50, CH_2CH_3), 1.90 (t of q (∼sext), 4H, J = 7.50, CH_2CH_3), 1.24 (d, 12H, J = 2.65, P$(CH_3)_2$), 1.06 (t, 6H, J = 7.43, CH_2CH_3), 0.92 (t, 6H, J = 7.47, CH_2CH_3); $^{13}C\{^1H\}$ NMR (CD_2Cl_2) 159.71, 157.49, 138.25 (d, J_{C-P} = 6.4, C_{Ar}−P), 135.49, 135.08, 132.94, 132.70, 129.43, 123.77, 78.87, 78.53, 32.78, 25.31, 25.00, 16.65 (d, J_{C-P} = 13.0, CH_3−P), 12.38, 11.62, 2.64; ^{31}P NMR (CD_2Cl_2) −44.50 (s); MS (EI) 712 (M^+).

5,17-Bis(diisopropylphosphino)-25,26,27,28-tetra-*n*-propoxycalix[4]arene (5b) (Cone). The reduction procedure was the same as that used for **5a** using **4b** as starting material. A white solid was obtained in quantitative yield (100%): T_m = 135−136 °C; ^1H NMR (CD_2Cl_2) 7.21 (d, 4H, J = 6.68, Ph), 6.14 (t, 2H, J = 7.49, Ph), 6.04 (d, 4H, J = 7.35, Ph), 4.44 (d, 4H, J = 13.28, ArCH_2), 4.04 (t, 4H, J = 8.25, OCH_2), 3.65 (t, 4H, J = 6.66, OCH_2), 3.14 (d, 4H, 13.35, ArCH_2), 2.12 (m, 4H, P$CH(CH_3)_2$), 1.91 (m, 8H, CH_2CH_3), 1.11 (dd, 12H, J = 6.96, PCH(CH_3)$_2$), 1.10 (t, 6H, J = 7.45, CH_2CH_3), 0.98 (dd, 12H, J = 6.84, PCH(CH_3)$_2$), 0.89 (t, 6H, J = 7.45, CH_2CH_3); $^{13}C\{^1H\}$ NMR (CD_2Cl_2) 159.32, 155.57, 137.00 (d, J_{C-P} = 8.1, C_{Ar}−P), 135.72, 135.46, 127.62, 122.32, 77.41, 76.85, 31.28, 23.96, 23.67 (d, J_{C-P} = 14.8, $(CH_3)_2CH$−P), 20.48, 20.23, 19.24, 19.13, 11.10, 10.00; $^{31}P\{^1H\}$ NMR (CD_2Cl_2) 12.95 (s); MS (EI) 825 (M^+).

Bis[*μ*-bis(5,17-bis(dimethylphosphino))-25,26,27,28-tetra-*n*-propoxycalix[4]arene)(1,5-cyclooctadiene)rhodium(I)] Hexafluorophosphate (6a). A solution of $TlPF_6$ (18.7 mg, 53.4 *μ*mol) and $[RhCl(COD)]_2$ (12.0 mg, 24.3 *μ*mol) in 8 mL of dry THF was stirred for 1 h at room temperature. Then, a solution of compound **5a** (34.5 mg, 48.5 *μ*mol) in THF was slowly added dropwise (for 1 h) to the previous rhodium solution. The solution was stirred for an additional 16 h. Then, the solution was filtered, and the solvent was evaporated. An orange solid was obtained in 90% yield (46.6 mg): T_m > 145 °C (dec); IR (neat solid) $\nu(PF_6^-)$ = 837 cm^{-1}; ^1H NMR (CD_2Cl_2) 7.22 (d, 4H, J = 7.39, Ph), 7.01 (t, 2H, J = 7.36, Ph), 6.03 (br m, 4H, Ph), 4.96 (br m, 4H, =CH COD), 4.45 (d, 4H, J = 13.85, ArCH_2), 3.98 (t, 4H, J = 6.11, OCH_2), 3.66 (t, 4H, J = 6.56, OCH_2), 3.17 (t, 4H, J = 13.9, ArCH_2), 2.37 (br m, 8H, CH_2 COD), 1.85 (br m, 8H, CH_2CH_3), 1.15−1.4 (br m, 12H, P$(CH_3)_2$), 1.11 (t, 6H, J = 7.37, CH_2CH_3), 0.86 (t, 6H, J = 7.51, CH_2CH_3); $^{31}P\{^1H\}$ NMR (CD_2Cl_2) −6.71 (d, Pcalix, J_{P-Rh} = 144), −141.13 (sept, PF_6^-, J_{P-F} = 710); MS (MALDI-TOF) 815 (100%, (CalixP$_2$)Rh), 923 (30%, (CalixP$_2$)Rh(COD)), 1560 (5%, (CalixP-(O)P)]$_2$Rh), 1771 (10%, (CalixP$_2$)Rh$_2$PF_6). Anal. Calcd for $C_{52}H_{70}O_4F_6P_3Rh$: C, 58.43; H, 6.60. Found: C, 58.35; H, 6.59.

Bis[*μ*-bis(5,17-bis(diisopropylphosphino))-25,26,27,28-tetra-*n*-propoxycalix[4]arene)(1,5-cyclooctadiene)rhodium(I)] Hexafluorophosphate (6b). This compound was prepared according to the same procedure as described for **6a** using **5b** diphosphine as starting material. An orange solid was obtained in 90% yield (51.4 mg): T_m > 160 °C (dec); IR (neat solid) $\nu(PF_6^-)$ = 838 cm^{-1}; ^1H NMR (acetone-d_6) 7.39 (d, 4H, J = 7.87, Ph), 6.09 (m, 6H, Ph), 5.25 (br m, 4H, =CH COD), 4.48 (d, 4H, J = 13.36, ArCH_2), 4.12 (t, 4H, J = 8.07, OCH_2), 3.67 (t, 4H, J = 6.59, OCH_2), 3.49 (br m, 4H, CH_2 COD), 3.29 (d, 4H, J = 13.41, ArCH_2), 2.79 (sext, 4H, J = 8.95, P$CH(CH_3)_2$), 2.37 (br m, 4H, CH_2 COD), 2.04−1.82 (m, 8H, CH_2CH_3), 1.51 (d, 6H, J = 7.06, PCH(CH_3)$_2$), 1.46 (d, 6H, J = 7.08, PCH(CH_3)$_2$), 1.31 (d, 6H, J = 6.93, PCH(CH_3)$_2$), 1.26 (d, 6H, J = 6.91, PCH(CH_3)$_2$), 1.13 (t, 6H, J = 7.37, CH_2CH_3), 0.91 (t, 6H, J = 7.42, CH_2CH_3); $^{31}P\{^1H\}$ NMR (acetone-d_6) 43.98 (d, Pcalix, J_{P-Rh} = 149), −137.65 (sept, PF_6^-, J_{P-F} = 704); MS (MALDI-TOF) 927 (100%, (CalixP$_2$)Rh), 1069 (15%, (CalixP$_2$)Rh(COD)), 1175 (5%, (CalixP$_2$)Rh$_2$PF_6, 1281 (15%, (CalixP$_2$)Rh$_2$(COD)PF_6). Anal. Calcd for $C_{60}H_{88}O_4F_6P_3Rh$: C, 60.90; H, 7.50. Found: C, 60.49; H, 7.53.

Bis[*μ*-bis(5,17-bis(diphenylphosphino))-11,23-dibromo-25,26,27,28-tetra-*n*-propoxycalix[4]arene)(1,5-cyclooctadiene)rhodium(I)] Hexafluorophosphate (6c). This compound was prepared according to the same procedure as described for **6a** using the **5c** diphosphine as starting material. An orange solid was obtained in 95% yield: T_m > 160 °C (dec); IR (neat solid) $\nu(PF_6^-)$ = 837 cm^{-1}; ^1H NMR (acetone-d_6) 7.4−7.9 (m, 22H, Ph), 7.36 (d, 2H, J = 12.0, Ph), 6.61 (s, 2H, PhBr), 4.48 (d, 4H, J = 13.5, ArCH_2), 4.0−4.25 (br m, 2H), 4.06 (t, 2H, J = 7.5, OCH_2), 3.83 (t, 2H, J = 7.0, OCH_2), 3.5−3.7 (br m, 2H), 3.30 (d, 4H, J = 13.5, ArCH_2), 2.4−2.6 (br m, 2H), 1.8−2.2 (m, 8H, CH_2CH_3), 0.8−1.2 (m, 8H, CH_3); $^{31}P\{^1H\}$ NMR (acetone-d_6) 30.04 (d, Pcalix, J_{P-Rh} = 145), −137.62 (sept, PF_6^-, J_{P-F} = 708); MS (MALDI-TOF) 1221 (100%, (CalixP$_2$)Rh), 1345 (35%, (CalixP$_2$)ORh(COD)), 2440 (1%, (CalixP$_2$)$_2$Rh$_2$)), 2552 (1%, (CalixP$_2$)Rh$_2$(COD)). Anal. Calcd for $C_{72}H_{76}Br_2O_4F_6P_3Rh$: C, 52.25; H, 4.63. Found: C, 52.19; H, 4.54.

5,11-Bis(dimethylphosphinoyl)-25,26,27,28-tetra-*n*-propoxycalix[4]arene (8a) (Cone). A solution of 100 mg (0.13 mmol) of **7** in 5 mL of dry THF at −78 °C was treated with a solution of 0.18 mL (0.30 mmol) of *t*-BuLi 1.7 M in hexane. The solution was stirred for 1 h at −78 °C, and 0.1 mL (0.65 mmol) of Me_2PCl was added. The solution was stirred for an additional 20 h and was allowed to reach room temperature. Then 0.1 mL (0.88 mmol) of hydrogen peroxide (30% in water) was added, and the mixture was stirred for 1 h. The solvent was then evaporated, and the yellow residue was purified using column chromatography under inert atmosphere using a 10:90 ethanol/$CHCl_3$ mixture (R_f = 0.21). A white solid was obtained. Yield: 25%; T_m = 110−112 °C; IR (neat solid) ν(P=O) = 1206 cm^{-1}; ^1H NMR ($CDCl_3$) 7.02 (d, 2H, J = 11.77, Ph), 6.95 (d, 2H, J = 11.76, Ph), 6.67−653 (m, 4H, Ph), 4.50 (d, 1H, J = 13.48, ArCH_2CH_2), 4.46 (d, 2H, J = 13.08, CH_2), 4.41 (d, 1H, J = 12.83, CH_2), 3.96−3.76 (m, 8H, OCH_2), 3.24 (d, 1H, J = 10.35, CH_2), 3.20 (d, 2H, J = 13.68, ArCH_2), 3.15 (d, 1H, J = 14.23, CH_2), 1.92 (t of q, 8H, CH_2CH_3), 1.52 (d, 6H, J_{P-H} = 3.50, P$(CH_3)_2$), 1.47 (d, 6H, J_{P-H} = 3.48, P$(CH_3)_2$), 0.99 (m, 12H, CH_2CH_3); $^{13}C\{^1H\}$ NMR ($CDCl_3$) 159.32, 156.42, 135.99 (d, J_{C-P} = 13.1, C_{Ar}-P), 135.11, 134.28, 129.98, 129.89, 129.25, 129.14, 128.31, 128.02, 122.48, 77.11, 77.00, 30.91, 23.16, 18.57, 17.47, 10.09; $^{31}P\{^1H\}$ NMR ($CDCl_3$)

35.40 (s); MS (FAB) 745 (M^+). Anal. Calcd for $C_{44}H_{58}O_6P_2$: C, 70.95; H, 7.79. Found: C, 70.96; H, 7.84.

5,11-Bis(diisopropylphosphinoyl)-25,26,27,28-tetra-*n*-propoxycalix[4]arene (8b) (Cone). This compound was prepared according to the same procedure described for **8a** using *i*-Pr_2PCl as phosphinating agent. A white solid was obtained. Yield: 45%; T_m = 106−108 °C; IR (neat solid) ν(P=O) = 1206 cm^{-1}; ^1H NMR ($CDCl_3$) 7.08 (d, 2H, J = 9.59, Ph), 7.01 (d, 2H, J = 5.42, Ph), 6.70 (br m, 4H, Ph), 6.55 (t, 2H, J = 7.40, Ph), 4.50 (d, 1H, J = 12.89, ArCH_2), 4.48 (d, 2H, J = 12.83, ArCH_2), 4.44 (d, 1H, J = 12.72, ArCH_2), 3.87 (m, 8H, OCH_2), 3.25 (d, 1H, J = 13.07, ArCH_2), 3.25 (d, 2H, J = 12.98, ArCH_2), 3.16 (d, 2H, J = 12.82, ArCH_2), 2.11 (sept, 4H, J = 7.41, P$CH(CH_3)_2$), 1.98 (t of q (∼sext), 8H, J = 7.50, $CH_2CH_2CH_3$), 1.04−0.73 (m, 36H, $PCH(CH_3)_2$ + $CH_2CH_2CH_3$); $^{13}C\{^1H\}$ NMR ($CDCl_3$) 158.86, 155.93, 135.17, 134.70, 134.30 (d, J_{C-P}=12.9, C_{Ar}-P), 132.30, 131.30, 128.31, 127.92, 122.67, 77.35, 76.50, 30.85, 30.73, 25.15, 24.25, 23.10 (d, J_{C-P} = 14.7, $(CH_3)_2CH$−P), 15.91, 15.73, 14.71, 10.12; $^{31}P\{^1H\}$ NMR (CD_2Cl_2) 52.40 (s); MS (FAB) 857 (M^+). Anal. Calcd for $C_{52}H_{74}O_6P_2$: C, 72.88; H, 8.64. Found: C, 72.77; H, 8.71.

5,11-Bis(dimethylphosphino)-25,26,27,28-tetra-*n*-propoxycalix[4]arene (9a) (Cone). A 40 mg (0.056 mmol) sample of **8a** was dissolved in 5 mL of toluene under inert atmosphere. The solution was refluxed, and 0.2 mL (1.62 mmol) of phenylsilane was added. The solution was stirred and refluxed for 24 h. The solvent was then evaporated, and the crude product was purified using column chromatography under an inert atmosphere using a 5:95 ethyl acetate/hexane mixture (R_f = 0.37). A white, oily product was obtained. Yield: 103%, 40 mg; T_m = 133−134 °C; ^1H NMR (CD_2Cl_2) 6.72 (d, 4H, J = 7.42, Ph), 6.64−6.53 (m, 6H, Ph), 4.44 (d, 1H, J = 13.23, ArCH_2), 4.43 (d, 3H, J = 13.20, ArCH_2), 3.85 (t, 4H, J = 7.15, OCH_2), 3.83 (t, 4H, J = 6.87, OCH_2), 3.17 (d, 1H, J = 13.23, ArCH_2), 3.14 (d, 3H, J = 13.25, ArCH_2), 1.94 (t of q, 8H, J = 7.51, CH_2CH_3), 1.07−0.97 (m, 24H); $^{13}C\{^1H\}$ NMR (CD_2Cl_2) 157.23, 156.84, 135.31, 135.40 (d, J_{C-P} = 6.4, C_{Ar}−P), 131.44, 131.15, 130.72, 130.51, 128.47, 128.40, 122.36, 77.21, 31.15, 23.67, 23.61, 10.48; $^{31}P\{^1H\}$ NMR (CD_2Cl_2) −44.51 (s); MS (EI) 712 (M^+).

5,11-Bis(diisopropylphosphino)-25,26,27,28-tetra-*n*-propoxycalix[4]arene (9b) (Cone). The reduction procedure was the same as that used for **9a** using **8b** as starting material. A white solid was obtained in 99% yield: ^1H NMR (CD_2Cl_2) 6.84 (t, 2H, J = 5.22, Ph), 6.69 (d, 4H, J = 7.44, Ph), 6.56 (d, 4H, J = 7.39, Ph), 4.46 (d, 4H, J = 12.85, ArCH_2), 3.88 (dt, 8H, J = 8.03, OCH_2), 3.18 (d, 3H, J = 12.9, ArCH_2), 3.16 ((d, 1H, J = 12.9, ArCH_2), 2.00 (m, 8H, CH_2CH_3), 1.97 (m, 4H, P$CH(CH_3)_2$), 1.01 (dt, 6H, J = 7.37, CH_2CH_3), 0.89 (dd, 12H, J = 7.06, $PCH(CH_3)_2$), 0.69 (dt, 6H, J = 7.35, CH_2CH_3); $^{13}C\{^1H\}$ NMR (CD_2Cl_2) 157.32, 156.59, 135.22 (d, J_{C-P} = 8.4, C_{Ar}-P), 134.87, 134.63, 131.31, 128.57, 122.85, 77.48, 77.35, 31.23, 31.11, 23.68, 22.81 (d, J_{C-P} = 8.9, $(CH_3)_2CH$−P), 20.09, 19.84, 19.05, 18.82, 10.49; $^{31}P\{^1H\}$ NMR (CD_2Cl_2) 12.67 (s); MS (EI) 825 (M^+).

Bis[*μ*-bis(5,11-bis(dimethylphosphino))-25,26,27,28-tetra-*n*-propoxycalix[4]-arene)(1,5-cyclooctadiene)rhodium(I)] Hexafluorophosphate (10a). This compound was prepared according to the same procedure described for **6a** using the **9a** diphosphine as starting material. An orange solid was obtained in 90% yield: T_m > 123 °C (dec); IR (neat solid) $\nu(PF_6^-)$ = 836 cm^{-1}; ^1H NMR (CD_2Cl_2) 6.20−7.40 (br m, 10H, Ph), 4.7−5.0 (br m, 4H, =CH COD), 4.3−4.6 (br m, 4H, ArCH_2), 3.6−4.1 (br m, 8H, OCH_2), 3.00−3.40 (br m, 4H, ArCH_2), 2.20−2.50 (br m, 4H), 1.70−2.10 (br m, 12H), 0.70−1.40 (br m, 24H); $^{31}P\{^1H\}$ NMR (CD_2Cl_2) −1.33 (d, Pcalix, J_{P-Rh} = 144), −141.02 (septuplet, PF_6^-, J_{P-F} = 711); MS (MALDI-TOF) 815 (10%, ($CalixP_2$)Rh), 831 (70%, (CalixP(O)P)Rh) 939 (15%, (CalixP-(O)P)Rh(COD)) 1560 (50%, ($CalixP(O)P)_2$Rh). Anal. Calcd for $C_{52}H_{70}O_4F_6P_3Rh$: C, 58.43; H, 6.60. Found: C, 58.27; H, 6.70.

Bis[*μ*-bis(5,11-bis(diisopropylphosphino))-25,26,27,28-tetra-*n*-propoxycalix[4]arene)(1,5-cyclooctadiene)rhodium(I)] Hexafluorophosphate (10b). This compound was prepared according to the same procedure described for **6a** using the **9b** diphosphine as starting material. An orange solid was obtained in 70% (32.1 mg) yield: T_m >150 °C (dec); IR (neat solid) $\nu(PF_6^-)$ = 838 cm^{-1}; ^1H NMR (CD_2Cl_2) 6.93 (d, 4H, J = 8.53, Ph), 6.72 (m, 4H, Ph), 6.56 (br t, 2H, Ph), 5.21 (br m, 4H, =CH COD), 4.47 (d, 3H, J = 12.9, ArCH_2), 4.45 (d, 1H, J = 12.9, ArCH_2), 3.91 (m, 8H, OCH_2), 3.22 (m, 4H, ArCH_2), 2.33 (m, 8H, P$CH(CH_3)_2$ + COD), 1.96 (m, 12H, CH_2CH_3 + COD), 0.80−1.4 (br m, 36H, CH_2CH_3 + $PCH(CH_3)_2$); $^{31}P\{^1H\}$ NMR (CD_2Cl_2) 40.04 (d, Pcalix, J_{P-Rh} = 149), −137.35 (sept, PF_6^-, J_{P-F} = 709); MS (MALDI-TOF) 927 (90%, ($CalixP_2$)Rh), 1069 (100%, ($CalixP_2$)Rh(COD)), 1175 (50%, ($CalixP_2$)Rh_2PF_6, 1281 (70%, ($CalixP_2$)Rh_2(COD)PF_6). Anal. Calcd for $C_{60}H_{88}O_4F_6P_3$-Rh: C, 60.90; H, 7.50. Found: C, 60.89; H, 7.51.

Bis[*μ*-bis(5,11-bis(diphenylphosphino))-25,26,27,28-tetra-*n*-propoxycalix[4]-arene)(1,5-cyclooctadiene)rhodium-(I)] Hexafluorophosphate (10c). This compound was prepared according to the same procedure described for **6a** using the **9c** diphosphine as starting material. An orange solid was obtained in 95% yield: T_m > 170 °C (dec); IR (neat solid) $\nu(PF_6^-)$ = 837 cm^{-1}; ^1H NMR (acetone-d_6) 6.0−8.0 (br m, 32H, Ph), 4.2−4.7 (br m, 4H, ArCH_2), 4.2−4.0 (br m, 4H, OCH_2), 3.8−4.0 (br m, 4H, OCH_2), 2.9−3.5 (br m, 4H, ArCH_2), 2.3−2.5 (br m, 4H), 1.8−2.2 (br m, 8H, CH_2CH_3), 0.8−1.2 (br m, 8H, CH_3); $^{31}P\{^1H\}$ NMR (acetone-d_6) 33.25 (d, Pcalix, J_{P-Rh} = 146), −137.62 (sept, PF_6^-, J_{P-F} = 708); MS (MALDI-TOF) 1063 (100%, $CalixP_2$Rh), 1171 (15%, $CalixP_2$Rh(COD)), 1311 (40%, $CalixP_2Rh_2PF_6$), 1419 (90%, $CalixP_2Rh_2$(COD)PF_6). Anal. Calcd for $C_{72}H_{78}O_4F_6P_3Rh$: C, 57.76; H, 5.25. Found: C, 57.05; H, 5.33.

***trans,trans*-Bis[*μ*-bis(5,17-bis(diphenylphosphino)-11,-23-dibromo-25,26,27,28-tetra-*n*-propoxycalix[4]-arene)chlorocarbonylrhodium(I)] (12).** A solution containing $[RhCl(COD)]_2$ (47 mg, 0.18 mmol) in dry THF (20 mL) was bubbled with carbon monoxide for 2 min. A solution of compound **5c** (200 mg, 0.18 mmol) in THF (8 mL) was added slowly (for 1 h) to the previous solution under agitation. The solution was stirred for 16 h. The solution was then concentrated (0.5 mL) under vacuum and was precipitated with ethyl ether. The solid obtained was filtered and was washed with ethyl ether (2 mL). A beige solid was obtained in 95% yield (0.23 g): T_m > 160 °C (dec); IR (neat solid) ν(CO) 1979 cm^{-1}; ^1H NMR (benzene-d_6) 8.18 (d, 2H, J = 8.5, Ph), 8.15 (d, 2H, J = 7.5, Ph), 7.93 (d, 2H, J = 10.0, Ph), 7.32−7.38 (m, 12H, Ph), 7.12−7.20 (m, 8H, Ph), 6.61 (s, 4H, PhBr), 4.14 (d, 4H, J = 13.5, ArCH_2), 3.86 (t, 4H, J = 8.5, OCH_2), 3.30 (t, 4H, J = 7.0, OCH_2), 2.78 (d, 4H, J = 13.5, ArCH_2), 1.77−1.85 (m, 4H, CH_2-CH_3), 1.54−1.61 (m, 4H, CH_2CH_3), 0.89 (t, 6H, J = 7.5, CH_3), 0.74 (t, 6H, J = 7.5, CH_3); $^{31}P\{^1H\}$ NMR (benzene-d_6) 29.46 (d, Pcalix, J_{P-Rh} = 128); MS MALDI-TOF 1221 (100%, ($CalixP_2$)-Rh), 1255 (30%, ($CalixP_2$)RhCl), 2339 (5%, $(CalixP_2)_2Rh$), 2408 (1%, $(CalixP_2)_2$Rh(CO)Cl), 2470 (5%, $(CalixP_2)_2Rh_2$(CO)), 2534 (1.3% $(CalixP_2)_2Rh_2(CO)_2$−Cl), 2570 (<1%, $(CalixP_2)_2Rh_2(CO)_2$-Cl_2). Anal. Calcd for $C_{65}H_{64}O_5P_2ClBr_2Rh$: C, 60.74; H, 5.02. Found: C, 60.59; H, 5.05.

***trans,trans*-Bis[*μ*-bis(5,11-bis(diphenylphosphino))-25,26,27,28-tetra-*n*-propoxycalix[4]arene)]chloro-carbonylrhodium(I)] (13).** This compound was prepared according to the same procedure described for **12** using the **9c** diphosphine as starting material. A beige solid was obtained in 95% yield: T_m > 170 °C (dec); IR (neat solid) ν(CO) 1980 cm^{-1}; ^1H NMR (benzene-d_6) 8.3−8.7 (br m, 4H, Ph), 6.0−8.0 (br m, 26 H, Ph), 4.59 (d, 4H, J = 13.0, $ArCH_2$), 4.29 (dd, 4H, J = 13.0, $ArCH_2$), 3.26 (d, 4H, J = 13.0, $ArCH_2$), 3.4 (br m, 8H, OCH_2), 1.5−2.0 (br m, 8H, CH_2CH_3), 0.6−1.0 (br m, 12H, CH_2CH_3);

$^{31}P\{^1H\}$ NMR (benzene-d_6) 30.62 (d, Pcalix, $J_{P-Rh} = 124$), 29.11 (d, Pcalix, $J_{P-Rh} = 129$); MS MALDI-TOF 2156 (100%, $(CalixP_2)_2Rh_2(CO)$), 2194 (95%, $(CalixP_2)_2Rh_2Cl_2$), 2289 (4%, $(CalixP_2)_2Rh_2(CO)Cl_2$. Anal. Calcd for $C_{65}H_{66}O_5P_2ClRh$: C, 69.24; H, 5.90. Found: C, 69.04; H, 6.11.

Bis[μ-bis(5,17-bis(diphenylphosphino))-11,23-dibromo-25,26,27,28-tetra-*n*-propoxycalix[4]arene)(1,5-cyclooctadiene)iridium(I)] hexafluorophosphate (14). To a solution of $[IrCl(COD)]_2$ (9 mg, 0.0134 mmol) in CH_2Cl_2 (2 mL) was added dropwise a solution of $TlPF_6$ (7.5 mg, 0.0295 mmol) in dry THF (1 mL). This orange solution was filtered over Celite and was added directly to a solution of **5c** (30 mg, 0.0268 mmol) in CH_2Cl_2 (8 mL). The solution was stirred for 1 h. After 1 h, the red solution was concentrated to ca. 3 mL and was precipitated with ethyl ether. The solution was filtered, and a pink solid was obtained in 65% yield (12.3 mg): $T_m > 190$ °C (dec); IR (neat solid) $\nu(PF_6^-) = 839$ cm^{-1}; ^1H NMR (CD_2Cl_2) 7.70−7.15 (m, 24H, Ph), 6.28 (s, 4H, PhBr), 4.58−4.49 (m, 4H, =CH COD), 4.39 (d, 4H, $J = 14.3$, ArCH_2), 4.08 (t, 4H, CH_2 COD), 3.59 (t, 8H, $J = 6.5$, O$CH_2CH_2CH_3$), 3.10 (d, 4H, $J = 14.3$, ArCH_2), 2.56−2.77 (m, 2H, CH_2 COD), 2.03−1.68 (m, 10H, $OCH_2CH_2CH_3$ + CH_2 COD), 1.04 (t, 6H, $J = 6.5$, $OCH_2CH_2CH_3$), 0.82 (t, 6H, $J = 6.5$, $OCH_2CH_2CH_3$); $^{31}P\{^1H\}$ NMR (CD_2Cl_2) 21.1 (s, PPh_2), −141.20 (sept, PF_6^-, $J_{P-F} = 708$). MS (FAB) 1311.2 (100%, $(CalixP_2)Ir$), 2430 (30%, $(CalixP_2)_2Ir$), 2538.2 (20%, $(calixP_2)_2Ir(COD)$). Anal. Calcd for $C_{72}H_{76}Br_2O_4F_6P_3Ir$: C, 49.58; H, 4.39. Found: C, 49.70; H, 4.28.

Bis[μ-bis(5,11-bis(diphenylphosphino))-25,26,27,28-tetra-*n*-propoxycalix[4]-arene)(1,5-cyclooctadiene)iridium-(I)] Hexafluorophosphate (15). This compound was prepared according to the same procedure described for **14** using the **9c** diphosphine as starting material. The solution was filtered, and a pink solid was obtained in 50% yield (12.3 mg): $T_m > 150$ °C (dec); IR (neat solid) $\nu(PF_6^-) = 839$ cm^{-1}; ^1H NMR (CD_2Cl_2) 7.61−5.79 (m, 30H, Ph), 4.66−4.31 (m, 8H, CH_2+ = CH COD), 4.35−3.61 (m, 12H, O$CH_2CH_2CH_3$ +COD), 3.42−2.82 (m, 4H, CH_2+ =CH COD), 2.12−1.59 (m, 12H, OCH_2CH_2-CH_3 +COD), 1.19−0.72 (m, 12H, $OCH_2CH_2CH_3$). $^{31}P\{^1H\}$ NMR (CD_2Cl_2) 21.1 (br s, PPh_2), −141 (sept, PF_6^-, $J_{P-F} = 709$); MS (FAB) 1153.3 (100%, $(CalixP_2)Ir$), 1453.7 (70%, $(CalixP_2)Ir_2$-(COD)), 1598.7 (35%, $(CalixP_2)Ir_2(COD)PF6$), 2114.4 (67%, $(CalixP_2)_2Ir$), 2222.9 (75%, $(CalixP_2)_2Ir(COD)$). Anal. Calcd for $C_{72}H_{78}O_4F_6P_3Ir$: C, 54.51; H, 4.95. Found: C, 54.41; H, 5.04.

***trans,trans*-Bis[μ-bis(5,17-bis(diisopropylphosphino))-25,26,27,28-tetra-*n*-propoxycalix[4]arene)hydridocarbonylrhodium(I)] (17).** A solution containing 20 mg (8.5 μmol) of **6b** in acetone (15 mL) was inserted in a high-pressure reactor heated at 50 °C. The reactor was purged three times with CO, then 35 atm of CO was applied, followed by 35 atm of H_2. The solution was stirred for 24 h, then allowed to cool to room temperature. The precipitate was filtered and washed with acetone. A white solid was obtained in 90% yield (15.0 mg): $T_m > 155$ °C (dec); IR (neat solid) ν(CO) 1970 cm^{-1}; ^1H NMR (CD_2Cl_2) 7.41 (m, 4H, Ph), 6.02 (m, 4H, Ph), 5.80 (t, 2H, $J = 7.62$, Ph), 4.43 (d, 4H, $J = 13.08$, ArCH_2), 4.09 (t, 4H, $J = 8.07$, OCH_2), 3.62 (t, 4H, $J = 6.69$, OCH_2), 3.16 (d, 4H, $J = 13.26$, ArCH_2), 2.94 (m, 4H, P$CH(CH_3)_2$), 2.05 (t of q (∼sext), 4H, $J = 7.69$, $OCH_2CH_2CH_3$), 1.87 (t of q (∼sext), 4H, $J = 7.17$, $OCH_2CH_2CH_3$), 1.34 (m, 12H, PCH(CH_3)$_2$), 1.20 (m, 12H, PCH-(CH_3)$_2$), 1.10 (t, 6H, $J = 7.35$, $OCH_2CH_2CH_3$), 0.93 (t, 6H, $J = 7.35$, $OCH_2CH_2CH_3$); $^{31}P\{^1H\}$ NMR (CD_2Cl_2) 45.55 (d, $J_{P-Rh} = 122$).

Hydroformylation Experiments. Hydroformylation reactions were performed in a 200 mL Parr Instrument autoclave (4001 model) equipped with a gas inlet−outlet valve and a liquid sampling valve. Mechanical stirring provided agitation. The autoclave was operating at 50 ± 1 °C. The reactor system was preheated to 50 °C before the experiment. A solution of rhodium dimer (5 μmol), 0.01 mol of substrates (alkenes), and 0.003 mol of methylcyclohexane (as internal standard) in THF was placed inside the reactor and allowed to reach the desired temperature in 20 min. The reactor was purged three times with CO gas. Then 35 atm of CO and 35 atm of H_2 was introduced into the reactor, while the stirring was activated. All the runs were 72 h long. Samples were removed regularly for GC/MS analysis through the sampling valve. The aldehyde products were analyzed by temperature-programmed gas chromatography (10 °C/min) from 60 to 250 °C with a DB-5MS column. A 0.9 mL/min helium flow was used. Tof is defined as the number of moles of products divided by the total number of moles of rhodium used per hour. In this work, [Rh] = 1×10^{-4} M. This latter value was used to calculate tof.

Computer Modeling. The calculations were performed using the commercially available PC-model from Serena Software (version 7.0), which uses the MMX empirical model. No constraints on bond distances or angles were applied to ensure that deviations from normal geometry are observed. Comparisons between literature X-ray structures and computed models are provided in the text.

Crystallography. Single crystals of **5b** were coated with Paratone-N oil, mounted using a glass fiber, and frozen in the cold nitrogen stream of the goniometer. A hemisphere of data was collected on a Bruker AXS P4/SMART 1000 diffractometer using ω and θ scans with a scan width of 0.3° and 30 s exposure times. The detector distance was 6 cm. The data were reduced (SAINT)[11] and corrected for absorption (SADABS).[12] The structure was solved by direct methods and refined by full-matrix least-squares on F^2 (SHELXTL).[13] Three of the propoxy groups were disordered, and the site occupancy was determined using an isotropic model as 0.75 (C(31)), 0.25 (C(31A)), 0.65 (C(32)−C(33), C(38)−C(39)) and 0.35 (C(32A)−C(33A), C(38A)−C(39A)) and fixed in subsequent refinement cycles. All non-hydrogen atoms were refined anisotropically. Hydrogen atoms were included in calculated positions and refined using a rigid model. Hydrogen atoms at C(31A), C(32A)−C(33A), and C(38A)−C(39A) were omitted. Thermal ellipsoid plots are at the 30% probability level. In some plots, hydrogen atoms have been omitted for clarity.

Results and Discussion

Syntheses and Characterization. The 1,2- and 1,3-diphosphinated ligands can be prepared in two steps from the corresponding dibromides **3** and **7**, or the tetrabromide **3b** (Schemes 1 and 2), using three different dichlorophosphine-starting materials (R_2PCl; R = Me, *i*-Pr, Ph). For the highly oxygen-sensitive phosphines (R = Me, *i*-Pr), hydrogen peroxide is added to syntheses, allowing the fully oxidized species to be formed (**4a**, **4b**, **8a**, **8b**). These latter compounds lead to better separation and purification, and this extra step provides better yields. The subsequent reduction proceeds cleanly with phenylsilane.

During the course of this study, single crystals suitable for X-ray analysis were obtained for **5b** (Figure 1 and Supporting Information).[14] The data confirm the cone conformation and indicate a flattened structure in which the phosphine groups are placed away from each

(11) *SAINT 6.02*; Bruker AXS, Inc.: Madison, WI, 1997−1999.
(12) Sheldrick, G. *SADABS*; Bruker AXS, Inc.: Madison, WI, 1999.
(13) Sheldrick, G. *SHELXTL 5.1*; Bruker AXS, Inc.: Madison, WI, 1997.
(14) (a) X-ray data were obtained for **4a** but were not of sufficient quality for full analysis. The conclusions made for the structure of **5b** are the same for this compound. The data can be found in the Supporting Information. (b) While this paper was being submitted, another related structure, 5,17-bis(diphenylphosphinoyl)-25,26,27,28-tetrapropoxycalix[4]arene, has been reported. The structure resembles that of our own structures. See: Jeunesse, C.; Matt, D.; Jones, P. G.; Thoennessen, H. *Acta Crystallogr*. **2003**, *E59*, 428.

Scheme 1

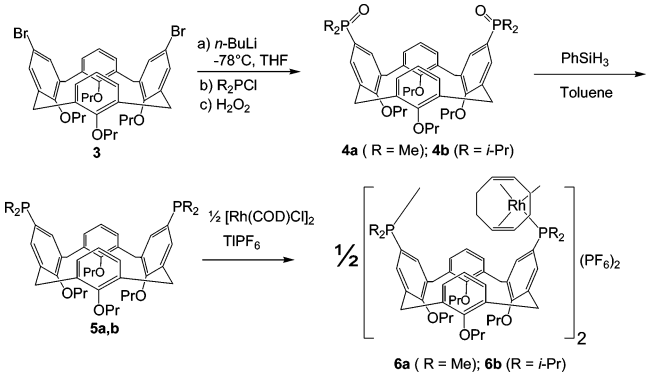

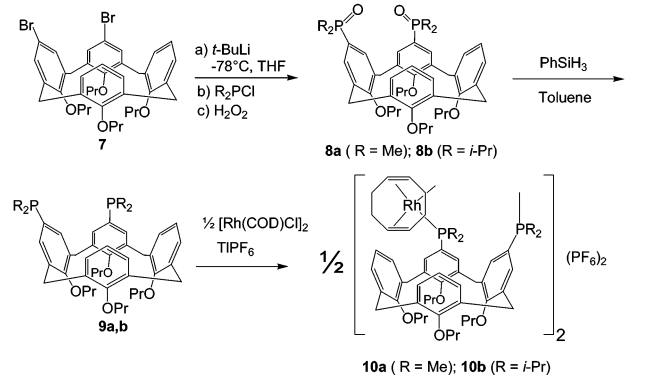

Scheme 2

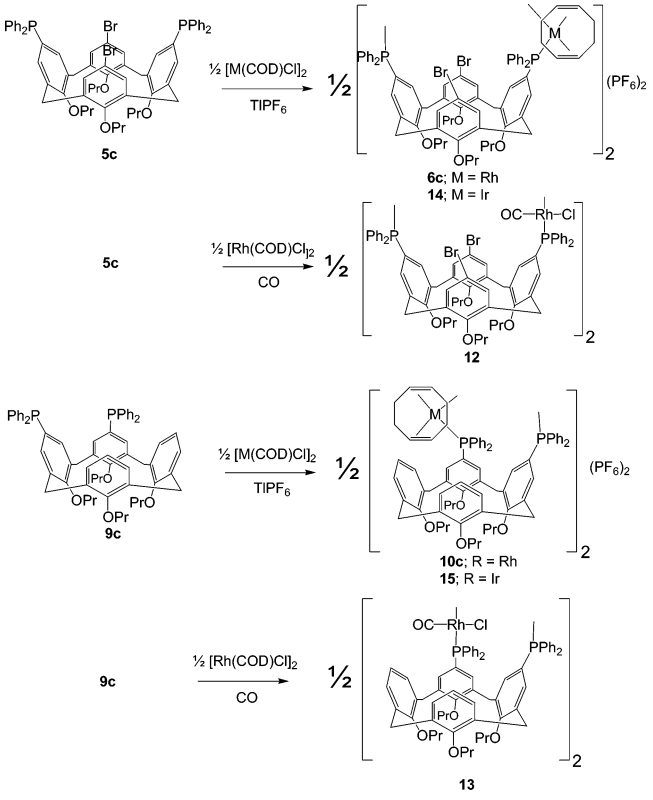

other, avoiding intramolecular steric interactions. The R_2P groups oriented such that the molecule has C_2-symmetry. The cavity is somewhat restricted in this solid state structure, where the nonbonding C···C

Figure 1. ORTEP drawing of the ligand **5b**. The ellipsoids are shown at 30% probability, and the H atoms are not shown for clarity.

Table 1. Comparison of Selected Nonbonded Distances for the X-ray and Modeled Structure of 5b

distance	X-ray/Å	computed/Å
inward C_{para}···C_{para}	4.080	4.725
outward C_{para}···C_{para}	10.253	10.277
inward O···O	5.943	5.974
outward O···O	3.380	3.789
P···P	13.360	13.360

distances are 4.342, 4.080, and 4.350 Å for the face-to-face C_{meta}···C_{meta}, C_{para}···C_{para}, and C_{meta}···C_{meta} separations, respectively, leading to an inward tilt of ∼15°. The two face-to-face O···O distances are 3.380 and 5.943 Å for outward and inward tilts, respectively. The wide C_{para}···C_{para} and P···P separations are 10.253 and 13.360 Å, respectively. The solution ^{1}H, ^{13}C, and ^{31}P NMR spectra are consistent with a 2-fold symmetry. The comparison of this experimental structure with a modeled one shows a good agreement (Table 1).

The coordination with the $Rh(COD)^+$ fragment onto the diphosphine ligands (**6a**,**b**,**c** and **10a**,**b**,**c**) proceeds in good yields (70−95%) with the use of the dimer bis-[chloro(1,5-cyclooctadienyl)rhodium(I)] reactant. The complexes did not provide single crystals suitable for X-ray crystallographic analysis. The MALDI-TOF data exhibit peaks that are attributable to fragments larger than a monomer (i.e., two or more calix[4]arene ligands). The analysis shows no evidence of chloride ion or rhodium chloride fragment in the sample. This result contrasts with the proposed related complex of the species 5,17-bis(methylene(diphenylphosphino))-25,26,-27,28-tetrapropoxycalix[4]arene,[15] in which two coordinated RhCl(COD) fragments are proposed to be dangling from the calix[4]arene upper rim. In this latter case, the preparation method differs from this one by not using $TlPF_6$ as a chloride-removing agent. The authors proposed a structure of the type $(PrO)_4$calix[4]-arene$[CH_2(Ph_2P)RhCl(COD)]_2$ (**11a**). In addition, the reaction of this same ligand with (COD)PdMeCl and $(COD)PtCl_2$ leads to polymers (or oligomers) of the type $(-calixP_2-PdMeCl-)_n$ (**11b**) and $(-calixP_2-PtCl_2-)_n$ (**11c**), as shown below, based on ^{1}H NMR spectra which exhibit broad signals.[15] In comparison with the 1,3-complexes reported here, the ^{1}H and ^{31}P NMR spectra

(15) Fang, X.; Scott, B. L.; Watkin, J. G.; Carter, C. A. G.; Kubas, G. J. *Inorg. Chim. Acta* **2001**, *317*, 276.

do not exhibit large signals at room temperature.

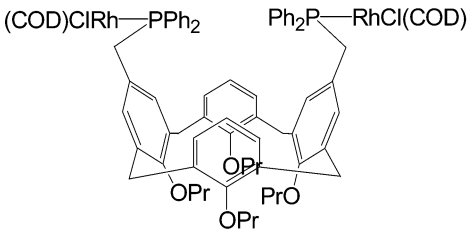

11a

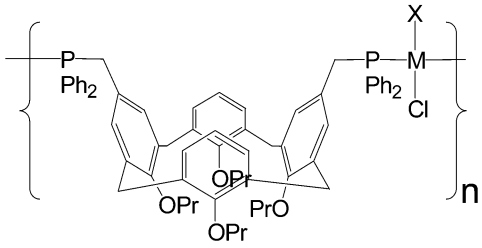

M = Pd; X = Me : **11b**
M = Pt; X = Cl : **11c**

In relation to the elucidation of the exact nature of the newly synthesized $Rh(COD)^+$ complexes, two RhCl(CO) complexes were also prepared (Scheme 2). Their syntheses proceed similarly to that of **6c** and **10c** with the difference that no Cl^- abstractor (such as Tl^+ or Ag^+) is added to the reaction under CO atmosphere. The complexes exhibit mass spectra (MALDI-TOF) where the molecular ion is observed for **12** and $[M - (CO)]^+$ for **13**, demonstrating their dimer nature in solution. The ^{31}P NMR spectra for **13** exhibit two very closely located signals with very similar J constants (J_{PRh}). These are possibly due to the two relative orientations of the Cl−Rh−CO axes (parallel and antiparallel) of the face-to-face Rh-coordination planes (the proposed structure is presented below). The complexes **12** and **13** are also neutral, and for T_1 measurements described below, this property is important. Their spectroscopic characterizations provide comparative data for the corresponding hydrides presented below.

Similarly to complexes **6c** and **10c**, the corresponding iridium(I) compounds (**14** and **15**) have been prepared in modest yields. The MALDI-TOF mass spectra also exhibit fragment peaks indicating the presence of dimers as well.

Spin−Lattice Relaxation Time Measurements. Due to the limited mass data for the $Rh(COD)^+$ species, the exact nature of the complexes in solution cannot be confidently addressed by this method. Moreover, due to the relatively weak solubility, the determination of the molecular weight using techniques such as the measurements of the freezing point depression cannot be applied. Recently, we demonstrated how spin−lattice relaxation time measurements can overcome these problems and provide information on the size of the tumbling molecules in solution.[16] This previous work reported in detail the methodology, and only the key features are presented here. The size (or volume) of a molecule can be obtained from the Stokes−Einstein−Debye equation assuming a spherical shape if the correlation time, τ_c, is known ($\tau_c = V\eta_{visc}/kT$; V = volume; η_{visc} = solvent viscosity; k = Boltzmann constant; T = temperature). To measure τ_c, one has to know the spin−lattice relaxation time related to dipole−dipole interactions, T_1^{DD}, which is given by the sum over all dipole−dipole interacting nuclei (^{31}P and ^1H in this work) according to eq 1:

$$1/T_1^{DD} = \sum(\hbar^2\gamma_P^2\gamma_H^2/4\pi^4 r_{PH}^6)\tau_c \qquad (1)$$

in the extreme narrowing limit,[17] where $\hbar$ is the Planck's constant, γ is the magnetogyric ratio for the interacting nuclei, and r is the distance between the probe nuclei (here ^{31}P) and the nearest interacting nuclei (here ^1H).[18] The T_1^{DD} data (here at 300 MHz ^1H) can be extracted from experimental T_1 and NOE measurements (nuclear Overhauser effect),[19] according to eq 2:

$$1/T_1^{DD} = \eta/(\eta_{max}T_1) \qquad (2)$$

with η = the fractional NOE constant, η_{max} = the maximum η value in the extreme narrowing limit (here $\eta_{max} = \gamma_H/2\gamma_P = 1.235$), and T_1 is the experimental spin−lattice relaxation time.[20] The strategy is to compare the hydrodynamic volume of a reliably known compound (crystallographically characterized monomer, dimer, or other) to that of the unknown ones. This standard molecule must be closely related to the sample ones. In this work, the probe nuclei is ^{31}P because it provides a better sensitivity than ^{13}C (natural abundance is 1%) and ^{103}Rh, for instance, and is free from interference (as in the ^1H spectra) since the signal is unique in the spectra. By combining eqs 1 and 2 to the Stokes−Einstein−Debye equation, one obtains

$$\frac{T_1(sam)}{T_1(sta)} = \frac{\eta_{PH}(sam)}{\eta_{PH}(sta)}\frac{V(sta)}{V(sam)}\frac{\sum 1/r_{PH}^6(sta)}{\sum 1/r_{PH}^6(sam)} \qquad (3)$$

where sam and sta stand for sample and standard, respectively. This equation requires the knowledge of the interatomic distances between the ^{31}P and ^1H nuclei, and η_{PH}. The X-ray structure presented for compound **5b** above provides such distances (Scheme 3).[21] By using the corresponding ligand as a standard, the term $[\sum 1/r_{PH}^6(sta)]/[\sum 1/r^6{}_{PH}{}^6(sam)]$ becomes unity. Because the chemical environment of the probe nucleus is the same

(16) Turcotte, M.; Harvey, P. D. *Inorg. Chem.* **2002**, *41*, 2971.

(17) T_1 decreases with the field (H_0), indicating the extreme narrowing limit.

(18) The interactions between the ^{103}Rh and ^{31}P, despite a shorter distance (2.27 Å according to literature X-ray data on related systems), account only for 1% or less of the total contribution on T_1^{DD} because of the small value for γ_{Rh} (9.442 MHz at 7.0463*T*; i.e., $\gamma_P = 121.442$ and $\gamma_H = 300.000$). See the cover table in Drago R. S. *Physical Methods for Chemists*, 2nd ed.; Saunders College Publishers: New York, 1992. These interactions were neglected in this work.

(19) Wehrli, F. W.; Wirthlin, T. *Interpretation of Carbon-13 NMR Spectra*; Heyden: London, 1980.

(20) The contribution from chemical shift anisotropy, quadrupolar, electron paramagnetic, chemical exchange, and spin−rotation processes are negligible. Indeed, the complexes do not exhibit quadrupolar nuclei nor are they paramagnetic. Although COD is considered labile, no evidence for efficient chemical exchange was seen in these complexes in the absence of other free ligands. The full-width at half-maximum (fwhm) was not strongly temperature dependent between 20 and 40 °C. Because of the sixth power of r in eq 1, any longer P···H distances generate terms that contribute less than 1% of T_1^{DD}.

(21) The X-ray data for **4a**, as well as the calculated structures, give similar values.

Table 2. T_1 Data for the Standards 4a, 5b, and 5c and Complexes 6a, 6b, 6c, 10a, 10b, 10c, 12

compound	$T_1/\pm 0.2$ s	$T_{1(sam)}/T_{1(sta)}$	V^a/Å^3	$V_{(sta)}/V_{(sam)}{}^b$
free 1,3-$(Ph_2P)_2Br_2$ (**5c**)	4.2		1279	
[1,3-$(Ph_2P)_2Br_2Rh(COD)^+]_2$ (**6c**)	2.4	0.57	2904	0.44
[1,2-$(Ph_2P)_2Rh(COD)^+]_2$ (**10c**)	2.2	0.53	2746	0.46
[1,3-$(Ph_2P)_2Br_2PRh(CO)Cl]_2$ (**12**)	1.8	0.43	2665	0.48
free 1,3-$(i\text{-}Pr_2P)_2$ (**5b**)	3.8		1121	
[1,3-$(i\text{-}Pr_2P)_2Rh(COD)^+]_2$ (**6b**)	2.0	0.53	2394	0.47
[1,2-$(i\text{-}Pr_2P)_2Rh(COD)^+]_2$ (**10b**)	1.6	0.42	2411	0.46
free 1,3-$(Me_2P{=}O)_2$ (**4a**)^c	2.6		978	
[1,3-$(Me_2P)_2Rh(COD)^+]_2$ (**6a**)	1.5	0.57	2073	0.47
[1,2-$(Me_2P)_2Rh(COD)^+]_2$ (**10a**)	1.7	0.65	2140	0.46

[a] Volume computed from modeling data using solvent-free models. [b] The ratio $V_{(sta)}/V_{(sam)}$ computed from modeling data. [c] **5a** proved too air-sensitive despite the precautions and oxidized too easily, even during measurements. Instead, **4a** was used as standard.

Scheme 3

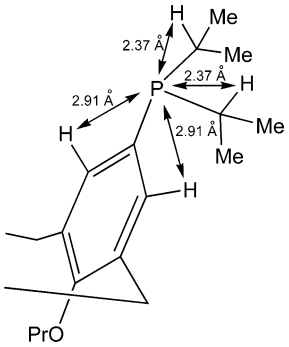

in the free and complexed ligands, η_{PH} are approximately the same, and the ratio $T_1(sam)/T_1(sta)$ is consequently approximately equal to that of $V(sta)/V(sam)$. In addition, the fact that the standard is neutral and the investigated complexes are monocations per unit of ligand, the hydrodynamic volume is anticipated to be greater for the charged species. For this reason, the related neutral complex 1,3-(PPh_2)calix[4]arene-[RhCl(CO)] (**12**) is also investigated to see the importance of this effect. This derivative, as well as the corresponding 1,2-isomer **13**, exhibits fragment peaks close to the dimer, or exactly on the dimer mass as stated above. The T_1 data are summarized in Table 2. The ratio $T_1(sam)/T_1(sta)$ is 0.43 for the neutral compound **12**, which compares favorably to the computed ratio $V(sta)/V(sam)$ for a dimer species (i.e., 0.48).[22] Other stoichiometries result in unacceptable ratios (1:1, 0.93; 1:3, 0.31; 1:4, 0.23). Clearly, only a dimer species can explain the T_1 data. For the charged species **6c** and **10c**, this ratio increases, indicating an increase in $V(sam)$. This result is consistent with the increase in hydrodynamic volume due to electrostatic interactions with the solvent.[23]

Comparison of the T_1 data between the free ligands **5c**, **5b**, and **4a** shows a decrease in this same order, which is consistent with an increase in the number of close ^1H nuclei for $^1H-^{31}P$ dipole−dipole interactions. This trend is also followed in the complexes as well. The average T_1 values for the 1,2- and 1,3-isomers are 2.3 > 1.8 > 1.6 s for the Ph_2P-, $i\text{-}Pr_2P-$, and Me_2P- derivatives, respectively. The $T_{1(sam)}/T_{1(std)}$ ratios indicate the presence of dimers in solution, for all the species.

Table 3. Comparison of the X-ray Data for 16 with Computed Structure[a]

distance	X-ray data/Å	computation/Å
Pd−P	2.319(5), 2.313(5)	2.37
Pd−Cl	2.323(4), 2.289(4)	2.19
Pd···Pd′	13.187(2)	13.35
P···P′	13.326(6)	13.39
$Cl\cdots Cl'_{outer}$	17.818(7)	17.63
$Cl\cdots Cl'_{inner}$	8.667(8)	9.17

[a] See ref 24.

Computer Modeling. The purpose of molecular modeling in this work is 2-fold. First, one may try to understand why dimerization occurs, and second, in the absence of X-ray data, what may be the steric hindrance about the metal in these species.

Prior to addressing these questions, the computational methodology has been tested on a ligand (see data for compound **5b** in Table 1) and on a crystallographically characterized related dimer compound, [1,3-$(Ph_2P)_2$-calixPd$Cl_2]_2$, recently published.[24] This dimer exhibits a large macrocycle composed of two face-to-face calix[4]arenes in a flattened structure. The comparison between the experimental and computed data (Table 3) is acceptable, where a discrepancy of approximately 0.1 and 0.2−0.5 Å for the M−L bond lengths and nonbonding separations, respectively, is noticed.

Computed monomer structures have been analyzed as well for comparison purposes. These monomer models exhibit computed P−Rh−P angles that are greater than the corresponding computed dimers discussed below. For instance, the 1,2-isomer computes a PRhP angle of 109° (instead of crystallographically found angles of 84° for other related species).[25] In addition, some of the aromatic rings show significant deviations from planarity, indicating clearly the presence of important ring stress in the monomer models. However, the ring stress in the 1,3-monomers is just only slightly greater than the corresponding dimers, where a difference of about 1−2° only in P−Rh−P angles are computed. This very small difference may explain why Matt and collaborators[8] have observed a monomer for the *trans*-$PtCl_2$ derivatives (**1**) and Takenaka et al.[24] have reported a

(22) The molecular volumes for **5b** and **5c** are 1121 and 1279 Å^3, respectively, according to the PC-Model. The X-ray data indicate a unit cell volume of 2550 Å^3 for **5b**, giving an approximated value of 1275 Å^3 for a single molecule, and 5753 Å^3 for $Z = 4$,[9] giving an approximated value of 1438 Å^3. This comparison is good taking into account the packing effect, which does not preclude an unavoidable void in the lattice. No solvent molecule was found as crystallizing molecule. By using the volume ratio, any systematic error caused by the method is minimized.

(23) No charged diphosphinated calix[4]arene complex species that are crystallographically characterized are available.

(24) Takenaka, K.; Obora, Y.; Jiang, L. H.; Tsuji, Y. *Organometallics* **2002**, *21*, 1158.

(25) Ball, R. G.; Payne, N. C. *Inorg. Chem.* **1977**, *16*, 1187.

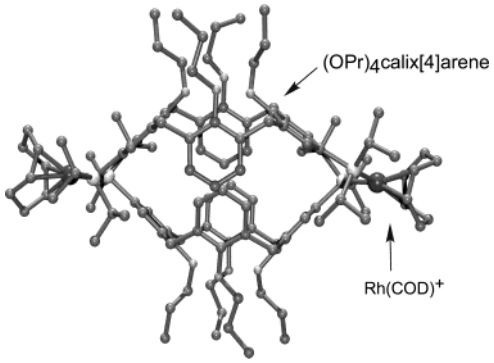

Figure 2. Model structure for **6b**.

Scheme 4

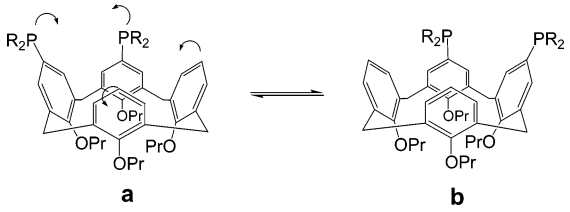

dimer for the *trans*-$PdCl_2$ species (**16**).

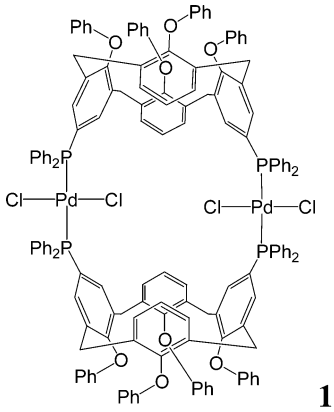

16

The 1,3-dimers can form only face-to-face species where the calix[4]arene macrocycles slightly sit in each other's cavities, forming an S-shape structure, with the C−H bonds penetrating the top of the cavity (Figure 2). Some degree of freedom is seen in the $Rh(COD)^+$ fragments where the $P_2Rh(C{=}C)_2$ planes may tilt up or down with respect to the bis(calix[4]arene) frame. Such motions involve the cooperativity of the R_2P groups. No Rh···Rh cooperativity can be anticipated as the Rh−Rh separation is on the order of 15 Å in this model. The calix[4]arene cavity is not available for interactions with substrates.

The analysis of the 1,2-dimers is more complicated. The ring flipping in the nonrigid calix[4]arene leads to two enantiomeric conformers, leading to two nonsuperimposable molecules due to the flattened geometry of the calix[4]arene (Scheme 4), which are called **a** and **b**. These species coexist in 50% population in solution, and the combinations of **a** + **a** (enantiomer), **b** + **b** (enantiomer), and **a** + **b** dimers during the coordination reactions are possible. However, the **a** + **a** and **b** + **b** forms are unlikely because the two macrocycles are placed side-by-side where both upper rims are directed in the same direction. In this geometry, the steric hindrance between the substituents is significant.

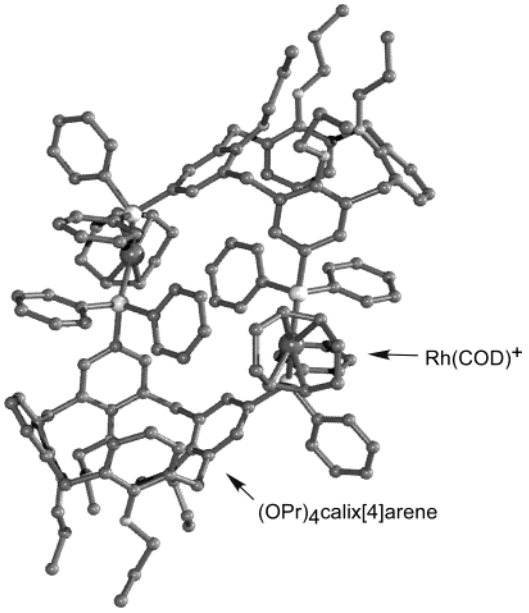

Figure 3. One possible model structure for **10c**, where the $Rh(COD)^+$ are away from each other.

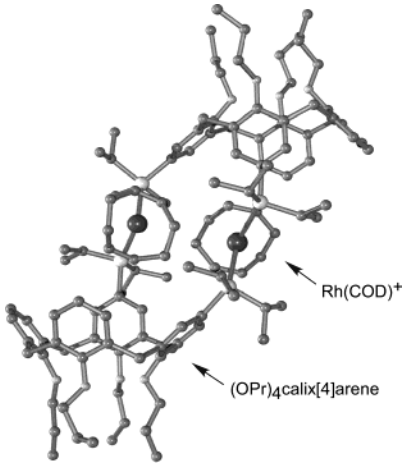

Figure 4. One possible model structure for **10c**, where the $Rh(COD)^+$ are located above the calix[4]arene cavity.

In the **a** + **b** form, the two calix[4]arene diphosphine ligands can be "turned around" with respect to each other where the tetrapropyl groups of one calix[4]arene are pointing in the opposite direction with respect to those of the second macrocycle. Then, three symmetric structures are still possible for this assemblage. First, the $Rh(COD)^+$ fragments can point away from each other (Figure 3) or can be trapped over the cavity (Figure 4). This latter structure is not without precedent, as Matt and collaborators have recently reported a structure of a bis(5,17-bis(diphenyl)diphosphino)calix[4]arene ruthenium(aryl) species where the aromatic group is located inside the cavity.[26] The third one places the $Rh(COD)^+$ groups toward each other and is physically impossible. In the two plausible models, the two main features are (1) the Rh···Rh separation is ∼8 Å for both cases and (2) the cavity is greatly obstructed either by the R_2P groups (R = Ph, *i*-Pr, Me) or by $Rh(COD)^+$ itself.

(26) Lejeune, M.; Jeunesse, C.; Matt, D.; Kyritsakas, N.; Welter, R.; Kintzinger, J. P. *J. Chem. Soc., Dalton Trans.* **2002** 1642.

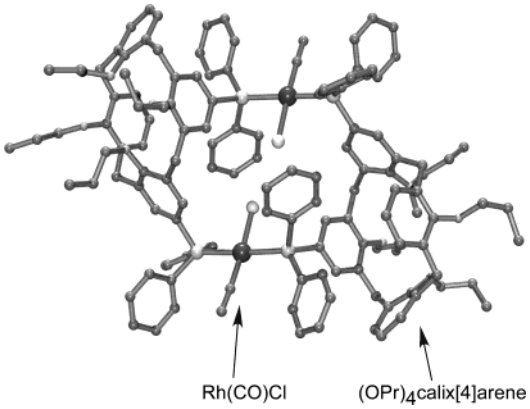

Figure 5. Model structure for **13**.

The side-by-side structures have been analyzed as well, and ring stress has readily been detected where calculated P−Rh−P angles > 96° are seen (instead of a theoretical value of 90°) and long Rh−P bond distances of 2.56 Å (instead of ~2.28 Å) are detected. In addition, important steric problems are noticed between the substituents of the four $-PR_2$ groups. Clearly, the side-by-side is not a favored geometry.

Compounds **12** and **13** have been modeled as well. In the 1,2-series, multiple conformers exist also, but fewer intramolecular steric interactions are noticed due to the *trans*-positions of the phosphine ligands. One of them (Figure 5) exhibits obstructed cavities by the R groups of the R_2P- fragments, leaving the ClRh(CO) unit well outside the macrocycle. The metallic centers appear completely accessible. The computed Rh····Rh separation is about 7.7 Å, which is the same as the P···P separations, and indicates the absence of direct interactions. The CPK models show also structures in which the ClRh(CO) groups can turn freely about the P···P′ axis when R = Me and *i*-Pr and requires some cooperation of the latter when R = Ph. The models investigated for the 1,3-isomers (see an example provided below for **17**) draw similar conclusions. In this case, the cavity is obstructed by the presence of the neighboring calix[4]arene, and the Rh atom is not obscured.

The major conclusion extracted from modeling is that the 1,2-diphosphinated calix[4]arene ligands clearly favor dimer structures and consequently the apical-apical coordination in the catalysis intermediates. In addition, because the Rh atoms are far apart in the dimer structure, their catalytic activities are probably uncorrelated. As for the 1,3-species, both monomer (chelate) and dimer (bridging) forms are possible, as little or no stress is demonstrated by modeling.

Interactions between 1-Hexene and 14 and 15. Photophysics is used to corroborate the structures for **6c** and **10c**. While the $Rh(COD)^+$ complexes investigated in this work are either nonluminescent or very weakly emissive, their corresponding iridium complexes (**14** and **15**) are phosphorescent at 77 K matrixes. A recent work from this group[27] has shown that it is possible to tell from the change in emission lifetime that interactions are present with the calix[4]arene-containing chromophore (see compounds **18** and **19**).

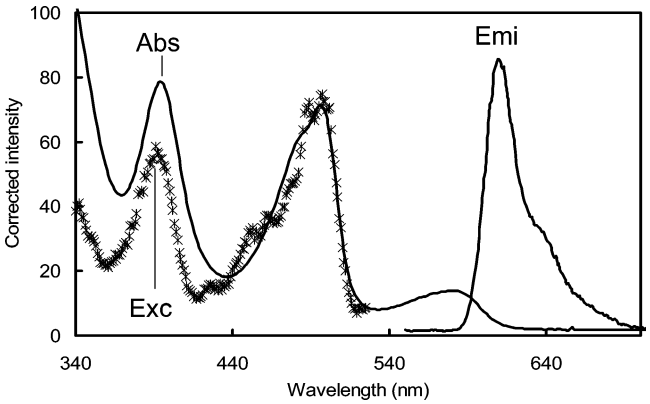

Figure 6. UV−vis (Ab), excitation (Ex), and emission (Em) spectra of **14** in ethanol at 77 K.

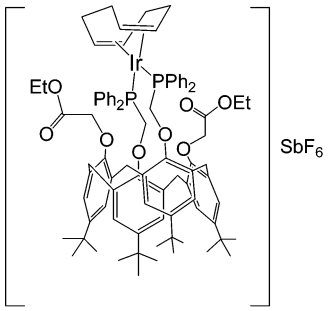

18

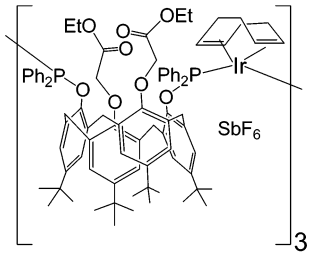

19

Figure 6 presents the room-temperature absorption spectrum of **14** as an example in the 340−640 nm range and exhibits the three characteristic absorptions known for the $P_2Ir(C{=}C)_2^+$ chromophore. These bands are located at 394, 496, and 580 nm, and similarly at 394, 496, and 578 nm for **15**. The lowest energy absorption band was previously assigned to a metal-to-ligand charge transfer (MLCT) from the iridium center to the olefins on the basis of EHMO and Heller's time-dependent theory.[27] Both complexes are luminescent in 77 K glasses, and their maxima are observed at 609 and 604 for **14** and **15**, respectively. The emission bands are weakly structured and exhibit excitation spectra that superimpose their corresponding absorption spectra. The emission lifetimes, τ_e, are 12.7 ± 0.2 and 11.4 ± 0.2 μs for **14** and **15**, respectively. These values indicate that the emissions arise from the ^{3}MLCT state and compare favorably to that found for the calix[4]arene $Ir(COD)^+$ species discussed above (13.5 ± 0.1 and 13.7 ± 0.1 μs for **18** and **19**).

Addition of 1-hexene at room temperature and immediately freezing the solution at 77 K induces two important changes. The first is a rapid decrease of the

(27) Gagnon, J.; Loeber, C.; Matt, D.; Harvey, D. P. *Inorg. Chim. Acta* **1996**, *242*, 137.

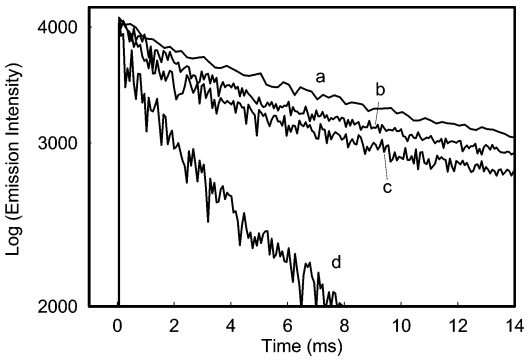

Figure 7. Comparison of the decay traces of the emission intensity for **14** in the presence of 1:0 (a), 1:10 (b), 1:100 (c), and 1:1000 (d) equivalents of 1-hexene in solution.

Scheme 5

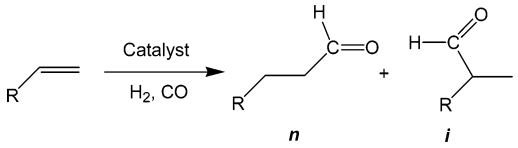

emission intensity with [1-hexene].[28] The second is a decrease in τ_e. Indeed, in both cases τ_e is sensitive to the amount of added 1-hexene, as exemplified in Figure 7. The data for **14** are 12.7, 7.8, 7.1, and <5 μs for ratios of 1:0, 1:10, 1:100, and 1:1000, and for **15**, 11.4, 11.0, 10.3, 7.4, and 6.4 μs for the above ratios in the same order (plus 1:5000 last datum).

The fact that τ_e decreases faster in **14** than in **15** with [1-hexene] indicates the greater relative steric hindrance in **15** about the chromophore center. These results corroborate the modeled structures presented in Figures 2−4.

Catalysis Properties. The homogeneous catalytic hydroformylations of five terminal olefins (Scheme 5) have been examined at 70 atm of 1:1 H_2/CO and 50 °C. These experimental conditions do not meet industrial standards, as the pressure is too high.[3a] The purpose of this study is to compare the performance for six catalysts over five substrates, which exhibit very different rates of reactivity. In addition, the larger tof's provide more sensitivity and a more accurate comparison. Moreover, at high pressure the risk of isomerization of 1-hexene into other isomers, which leads to other isomer products, is significantly smaller, as experimentally observed.

The generally accepted mechanism explaining the presence of *n*- (linear) and *i*- (branched) products is shown in Scheme 6.[5a,29] The $P_2Rh(COD)^+$ precursor is transformed into a monohydride carbonyl complex, which undergoes an addition with the free olefin. The key step is the insertion of the olefin into the Rh−H bond (migratory insertion). Depending on which carbon atom the hydride migrates to, two intermediates are possible, leading to the *n*- or *i*-products. Subsequently, addition of CO in the Rh coordination sphere promotes the carbonyl migration−insertion into the Rh−C bond. The final oxidative addition of H_2 on this intermediate produces a Rh(III) compound, which undergoes a reductive elimination to release the aldehyde compounds. For these dimers, the intramolecular steric factors deduced in the modeling of the *trans*-RhCl(CO) and $Rh(COD)^+$ (always *cis*-) species favor the apical-apical geometry for the intermediates.

In the absence of excess of free diphosphine, the reaction proceeds efficiently, as exemplified in Figure 8. The stability of the active catalysts was checked by UV−vis spectroscopy during the catalyses of all hydroformylation reactions of 1-hexene. This substrate was investigated because there is no optical interference in the absorption region of the catalysts. In all cases, the

Scheme 6

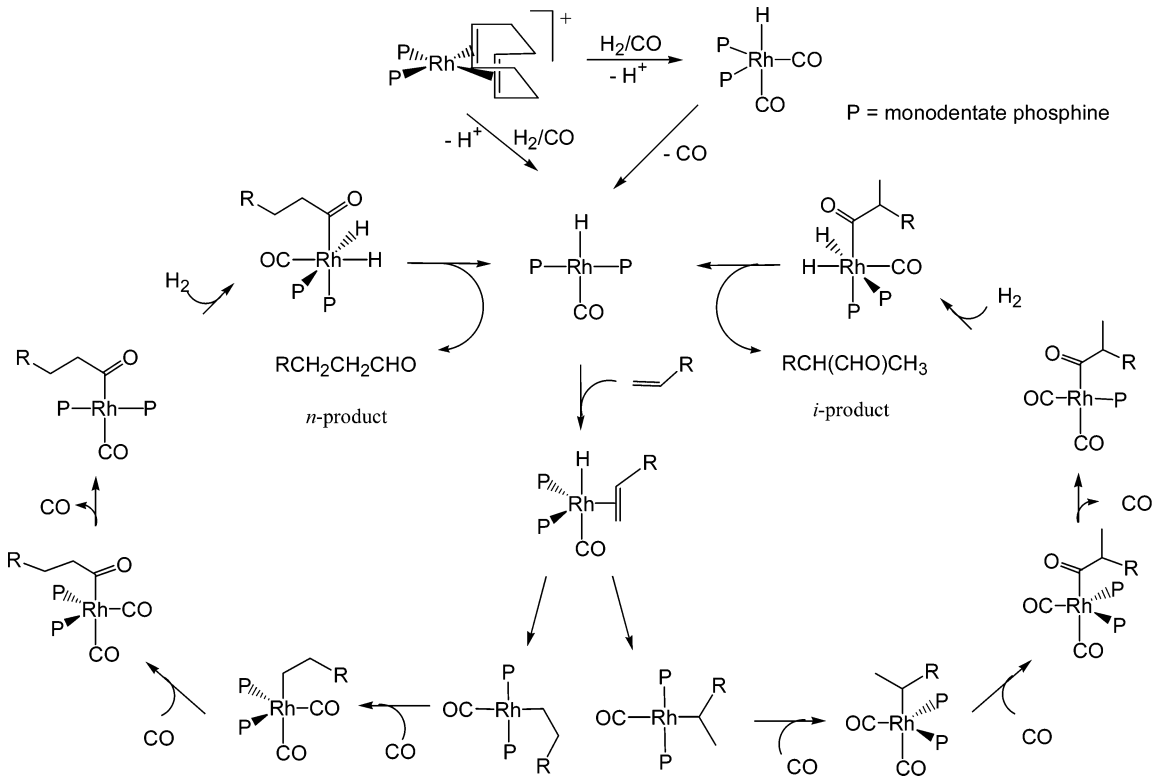

Table 4. Reaction Rates (tof) for the Catalyzed Hydroformylation Reactions Using 6a−c[a]

	6a			6b			6c		
substrate	reaction time (h)	conversion (±0.1%)	tof (h^{-1})	reaction time (h)	conversion (±0.1%)	tof (h^{-1})	reaction time (h)	conversion (±0.1%)	tof (h^{-1})
1-hexene	72	>99	51	30	>99	97	24	>99	141
styrene	72	58.9	35	30	>99	82	48	>99	80
vinyl acetate	72	35.2	5	48	>99	49	72	95.0	65
vinyl benzoate	72	82.2	14	48	>99	65	72	>99	66
vinyl *p-tert*-butylbezoate	72	21.8	3	48	>99	67	48	>99	94

[a] Conditions: $P = 70$ atm, $CO/H_2 = 1$, $T = 50$ °C, [alkene] = 0.1 M, [Rh] = 10^{-4} M (i.e., [**6a**,**b**,**c**] = 5×10^{-5} M). The reaction times were 72 h maximum. Any value different from 72 h indicates when the reaction was completed.

Table 5. Reaction Rates (tof) for the Catalyzed Hydroformylation Reactions Using 10a−c[a]

	10a			10b			10c		
substrate	reaction time (h)	conversion (±0.1%)	tof (h^{-1})	reaction time (h)	conversion (±0.1%)	tof (h^{-1})	reaction time (h)	conversion (±0.1%)	tof (h^{-1})
1-hexene	24	>99	106	24	>99	211	24	>99	250
styrene	72	37.9	11	48	>99	65	72	84.3	11
vinyl acetate	72	34.0	7	48	>99	41	72	55.8	8
vinyl benzoate	72	53.8	8	48	>99	63	72	>99	33
vinyl *p-tert*-butylbezoate	72	72.5	14	24	>99	78	72	>99	57

[a] Conditions: $P = 70$ atm, $CO/H_2 = 1$, $T = 50$ °C, [alkene] = 0.1 M, [Rh] = 10^{-4} M (i.e., [**10a**,**b**,**c**] = 5×10^{-5} M). The reaction times were 72 h maximum. Any value different from 72 h indicates when the reaction was completed.

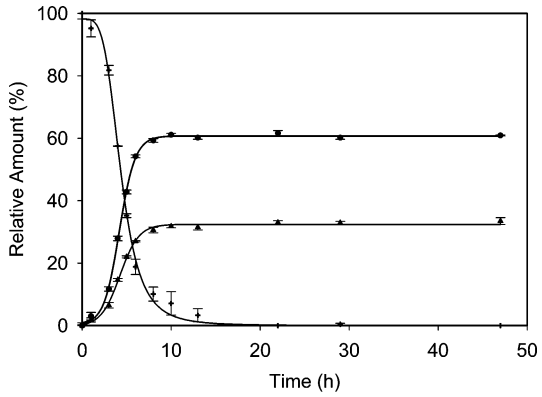

Figure 8. Evolution of the hydroformylation products for the catalysis of 1-hexene by **10b** (+ = 1-hexene, ● = 1-heptanal, ▲ = 2-methylhexanal).

UV−vis spectra in the 200−400 nm region were unchanged during the reactions for all the experimental conditions used.

The data show that for all six catalysts (Tables 4 and 5) the 1-hexene is clearly more reactive than the conjugated vinyls (greater tof), consistent with the nonstabilized olefin. Despite the different structure, the styrene substrate reacts with tof's in the same order of magnitude as the three other O-substituted vinyls.

The comparison of the tof data as a function of the catalyst indicates two features. For 1-hexene, both 1,3- and 1,2-precursors exhibit a trend in tof varying as Ph_2P- > *i*-Pr_2P- > Me_2P-. For the four other substrates, the 1,3- and 1,2-catalysts behave differently. For the 1,3-derivatives, the tof's vary as Ph_2P- ≥ *i*-Pr_2P- > Me_2P- as well, but the latter phosphine gives poorer results. For the 1,2-series, the tof's decrease as *i*-Pr_2P- > Ph_2P- ≥ Me_2P-, where both latter phosphines exhibit modest rates. Despite the relatively small size, the Me_2P- group does not lead to large tof, but exhibits better regioselectivity with respect to styrene and the O-substituted vinyl substrates.

Table 6. Regioselectivity (*n*/*i* ratio) for the Catalyzed Hydroformylation Reactions for the Catalysts 6a−c and 10a−c[a]

	n/*i* ratio (± 0.001)					
substrate	**6a**	**10a**	**6b**	**10b**	**6c**	**10c**
1-hexene	1.807	1.703	1.857	1.816	1.718	1.708
styrene	0.059	0.057	0.105	0.119	0.086	0.070
vinyl acetate	0.047	0.052	0.093	0.074	0.051	0.092
vinyl benzoate	0.006	0.005	0.006	0.003	0.008	0.005
vinyl *p-tert*-butylbenzoate	0.001	0.005	0.005	0.003	0.004	0.002

[a] Conditions: $P = 70$ atm, $CO/H_2 = 1$, $T = 50$ °C, [alkene] = 0.1 M, [Rh] = 10^{-4} M (i.e., [**6a**,**b**,**c**] and [**10a**,**b**,**c**]= 5×10^{-5} M).

The regioselectivities for the hydroformylation reactions are presented in Table 6. The data can be separated into two categories: first, 1-hexene, which exhibits a modest *n*/*i* ratio of ∼1.7−1.9; second, the conjugated vinyls for which 0.120 > *n*/*i* > 0.001. The better results are obtained for vinyl benzoate and *p-tert*-butylbenzoate, where the *n*/*i* ratios are <0.01 (i.e., *i*-selectivity greater than 99%), with the vinyl *tert*-butylbenzoate giving the better results. These observations are consistent with the models presented in Scheme 7.[3a] During the hydroformylation reaction, a metal−alkyl bond is formed during the insertion of the H atom onto the coordinated olefin (Scheme 6). In the alkyl-rhodium intermediates, this bond is polarized with a partial positive charge on the metal and a partial negative charge on the carbon (Scheme 7). When R is an aromatic group, the latter permits delocalization of

(28) The overall intensity decreases dramatically with [1-hexene] (a change that is greater than the change in lifetimes), so that efficient quenching occurs. Since energy transfer from the ^{3}MLCT to $^3\pi^*$ state of 1-hexene cannot operate (i.e., $E(^3\text{MLCT}) \ll E(^3\pi^*)$) and electron transfer from the same donor and acceptor cannot proceed (no sufficient driving force as the $E^{0/1-}(H_2C{=}CHR)$ is too large), only a ground state nonemissive (or weakly emissive) complex can explain this quenching, as no change in emission band shape is observed. One possible explanation is that 1-hexene displaces COD to form a nonluminescent species of the type $P_2Ir(1\text{-hexene})_2^+$. Additions of 1-hexene to Rh(COD)$^+$-containing solutions in 1:1 ratio exhibit ^{1}H NMR spectra where no free COD and 1-hexene are observed. This result indicates that these ligands undergo chemical exchange in solution. In **14** and **15**, such exchange also occurs, but at 77 K, the process is stopped and the solutions are composed of a mixture of the starting material in deceasing amount according to the increase in [1-hexene] and the nonluminescent species.

Scheme 7

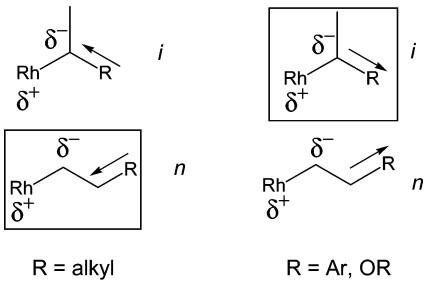

this partial negative charge at the *i*-position. Similarly, for electron-withdrawing groups such as acyls, inductive effects delocalize this partial charge at the *i*-position more than at the *n*-position. As a result, the *i*-isomer is strongly favored. When R is an electron donor group such as an alkyl group, no delocalization occurs for either isomer. These isomers appear as products in similar amounts, with the exception that the *i*-isomer is less favored due to an inductive effect. Despite the fact that these diphosphine ligands exhibit different basicity (the electronic parameters χ are 13.25, 10.60, and 7.50 cm^{-1}, for *i*-Pr_2P−, Ph_2P−, and Me_2P−, respectively)[30] and cone angles (155°, 145°, and 125°, respectively),[31] the *n*/*i* ratios vary only modestly.

Addition of 4 equiv of triphenylphosphine to the reaction mixture at 50 °C and 70 atm for the hydroformylation of 1-hexene using **6b** as an example, leads to a 2-fold decrease in tof. The reaction still goes to 97% completion after 48 h. This result indicates that the free phosphine competitively blocks the coordinating site about the rhodium center in the intermediate species, rather than stabilizing it. Similarly, the *n*/*i* ratio has been only modestly modified from 1.86 to 2.04 in these experiments.

Under soft conditions (P = 7 atm, T = 35 °C), compounds **6b** and **10b** also perform the catalytic hydroformylation of 1-hexene. At lower pressure, the isomerization of 1-hexene is possible, and other minor products are observed (less than 5% of the total amount of products, and were ignored in these present analyses). Their performances (tof) compare with the best most known rhodium catalysts (Supporting Information).[4a,7a,32] The best catalyst known so far is the BISBI-3,5-CF_3/$Rh(CO)_2$(acac) for both tof and *n*/*i*.[7a]

The comparison of the hydroformylation reaction of styrene is somewhat difficult to make because of different conditions used (Supporting Information),[2d,4c,5c,33−35] but it indicates that the species **6a**,**b**,**c** and **10a**,**b**,**c** are good catalysts. Compounds **6a** and **10a** are the best in this series, in particular in comparison with the second best catalyst for this substrate (Py-diphos/$Rh(CO)_2$(acac)). This comparison shows the inverse relationship between *n*/*i* ratios and tof.

The comparison of the catalytic performances for vinyl acetate with literature data (Supporting Information)[4c,6,34] also shows the better conversion rates and tof for **6b** and **10b** (as examples). However, *n*/*i* ratios are comparable, one average, with other systems.

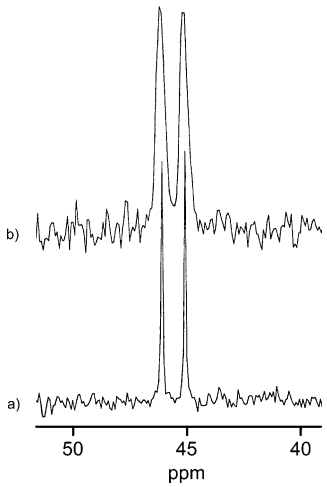

Figure 9. Comparison of the decoupled (a) and coupled (b) $\{^1H\}^{31}P$ NMR spectra of **17**.

Synthesis of Hydride 17. One hydride carbonyl complex (one suspected intermediate in the hydroformylation reactions) has been prepared from the corresponding $Rh(COD)^+$ precursors according to the same conditions applied for the catalyses:

$$\mathbf{6b} \xrightarrow[\text{THF/24 h}]{\text{50 °C/70 atm CO/H}_2} [1,3\text{-}(i\text{-}Pr_2P)_2\text{calixRh(H)(CO)}]_2\ (\mathbf{17}) \quad (4)$$

Complex **17** is characterized from ^1H NMR, ^{31}P NMR, and IR spectroscopy and T_1 measurements. The chemical shift (δ ^{31}P = 45.6 ppm) is consistent with a *i*-Pr_2P-Rh environment, and the coupling constant $^1J_{P-Rh}$ of 122.2 Hz is in line with a *trans* geometry. Compounds **12** and **13** exhibit similar constants (128 and 124 Hz, respectively). A strong peak at 1970 cm^{-1} evidences the presence of CO, and the T_1 measurements (T_1 = 1.4 s) indicate that the complex is a dimer in solution. The signals belonging to ligand COD are absent in the ^1H NMR spectra, and PF_6^- is absent as well according to both ^{31}P NMR and IR. However, the hydride signal has not been found yet. It is unclear whether it is too wide to be measured, or it is placed at an unusual shift and is lost under other ^1H signals.[36] Its presence can clearly be felt in two ways. First, the T_1 datum of 1.4 s is shorter than that of **6b**, the corresponding COD complex. This hydride adds an extra nuclei (S = 1/2) for dipole−dipole $^{31}P\cdots^1H$ interactions (distance ∼2.93 Å according to models, a distance similar to that of the aryl-$^1H\cdots^{31}P$ interactions; Scheme 3). Second, the coupled and decoupled $\{^1H\}^{31}P$ NMR spectra exhibit an important change in full-width at half-maximum (fwhm) (Figure 9). The fwhm are 53 and 14 Hz for the coupled and decoupled spectra, respectively. The ^{31}P couples with the

(29) Broussard, M. E.; Juma, B.; Train, S. G.; Peng, W.-J.; Laneman, S. A.; Stanley, G. G. *Science* **1993**, *260*, 784.
(30) Bartik, T.; Himler, T.; Schulte, H. G.; Seevogel, K. *J. Organomet. Chem.* **1984**, *272*, 29.
(31) Dias, P. B.; Minas de Piedade, M. E.; Simões, J. A. M. *Coord. Chem. Rev.* **1994**, *135/136*, 737.
(32) Hughes, O. R.; Unruh, J. D. *J. Mol. Catal.* **1981**, *12*, 71.
(33) Doyle, M. P.; Shanklin, M. S.; Zlokazov, M. V. *Synlett* **1994**, 615.
(34) Basoli, C.; Botteghi, C.; Cabras, M. A.; Chelucci, G.; Marchetti, M. *J. Organomet. Chem.* **1995**, *C20−22*, 488.
(35) Freixa, Z.; Pereira, M. M.; Pais, A. A. C. C.; Bayón, J. C. *J. Chem. Soc., Dalton Trans.* **1999**, 3245.
(36) In a recent work, the Pd−H signal was found at +5.1 ppm because of the proximity to the deshielding region of the aromatic phenyl rings. See: Meilleur, D.: Harvey, P. D. *Can. J. Chem.* **2001**, *79*, 552.

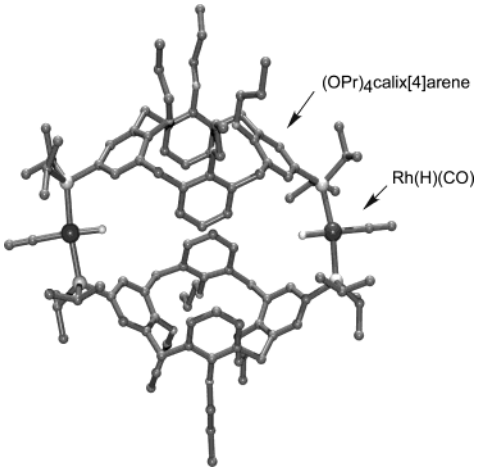

Figure 10. Model structure for **17**.

C*H*$(CH_3)_3$ nuclei as well. The coupling constant $^2J_{HP}$ is about 11 Hz, as seen in the doublet of septets for **4b** (the other compounds giving poorly resolved peaks). Taking into account the natural fwhm of decoupled spectra (coupling with ^{103}Rh excluded), the predicted fwhm is only 21 Hz. However, if a second $^2J_{PH}$ coupling occurs for the hydride, with a constant of ~30 Hz, then the predicted value (~51 Hz) would fit the experimental value (53 Hz). A small H−P coupling constant is consistent with a *cis* geometry.[7a] In addition, the fwhm for the ^{31}P NMR signal for **4b** is about 12 Hz, which compares well with the 14 Hz value extracted form the decoupled spectrum of **17**.

The computer modeling of **17** (Figure 10) also exhibits the face-to-face geometry. In comparison with **6b** (Figure 2), the calix[4]arene macrocycles are placed further from each other, but still space is available for a molecule to penetrate inside the large bis-calix[4]arene frame. Interactions between a substrate and the metal center can occur only on the outside of the dimer structure.

Final Remarks

The reported precursors are good catalysts for the hydroformylation reaction of terminal alkenes. The apical-apical geometry is highly probable in the hydroformylation intermediates, but there is no evidence for important differences in performance, better or worse, when one compares data with other catalysts in the literature. Within the list of precursors and substrates presented in this work, the choice of catalysts strongly depends on the desired performance and the specific alkene targets. By examining the best catalyst for 1-hexene for example as listed Table 6, dissymmetry within the ligand provides better selectivity. The syntheses of dissymmetric diphosphinated calix[4]arene ligands are not such a hard task and also still provide the opportunity to take advantage of a cavity if the structures are favorable.

Acknowledgment. This research was supported by the Natural Science and Engineering Research Council (NSERC). F.P. and J.G. thank the Université de Sherbrooke and NSERC, respectively, for scholarships.

Supporting Information Available: Tables listing detailed crystallographic data and structure refinement, atomic coordinates parameters and isotropic displacement parameters, bond lengths and angles, anisotropic displacement parameters, hydrogen coordinates and isotropic displacement parameters, torsion angles, and least-squares planes deviations, ORTEP figures for compounds **4a** and **5b**. Tables comparing tof and *n*/*i* ratios with literature for 1-hexene, styrene, and vinyl acetate. This material is available free of charge via the Internet at http://pubs.acs.org.

OM030095O